

1 Flood risk reduction and flow buffering as ecosystem services:

2 I. Theory on a flow persistence indicator for watershed health

3 Meine van Noordwijk^{1,2}, Lisa Tanika¹, Betha Lusiana¹

4 [1]{World Agroforestry Centre (ICRAF), SE Asia program, Bogor, Indonesia}

5 [2]{Wageningen University, Plant Production Systems, Wageningen, the Netherlands}

6 Correspondence to: Meine van Noordwijk (m.vannoordwijk@cgiar.org)

7

8 **Abstract 1**

9 We present and discuss a candidate for a single parameter representation of the complex
10 concept of watershed quality that does align short and long term responses, and provides
11 bounds to the levels of unpredictability. Flow buffering in landscapes is commonly
12 interpreted as ecosystem service, but needs quantification, as flood damage reflects
13 insufficient adaptation of human presence and activity to location and variability of river
14 flow in a given climate. Increased variability and reduced predictability of river flow is
15 a common sign, in public discourse, of degrading watersheds, combining increased
16 flooding risk and reduced low flows. Geology, landscape form, soil porosity, litter layer
17 and surface features, drainage pathways, vegetation and space-time patterns of rainfall
18 interact in complex space-time patterns of river flow, but the anthropogenic aspects tend
19 to get discussed on a one-dimensional scale of degradation and restoration, or in other
20 parts of the literature as due to climate change. A strong tradition in public discourse
21 associates changes on such degradation-restoration axis with binary deforestation-
22 reforestation shifts. Empirical evidence for such link that may exist at high spatial
23 resolution may not be a safe basis for securing required flow buffering in landscapes at
24 large. We define a dimensionless FlowPer parameter F_p that represents predictability of
25 river flow in a recursive flow model. Analysis suggests that buffering has two
26 interlinked effects: a smaller fraction of fresh rainfall enters the streams, and flow
27 becomes more persistent, in that the ratio of the flow on subsequent days has a higher
28 minimum level. As a potential indicator of watershed health (or quality), the F_p metric
29 (or its change over time from what appears to be the local norm) matches local
30 knowledge concepts, captures key aspects of the river flow dynamic and can be
31 unambiguously derived from empirical river flow data. Further exploration of
32 responsiveness of F_p to the interaction of land cover and the specific realization of space-
33 time patterns of rainfall in a limited observation period is needed to test the
34 interpretation of F_p as indicator of watershed health (or quality) in the way this is
35 degrading or restoring through land cover change and modifications of the overland and
36 surface flow pathways, given inherent properties such as geology, geomorphology and
37 climate.

38 **1 Introduction**

39 Degradation of watersheds and its consequences for river flow regime and flooding intensity
40 and frequency are a widespread concern (Brauman et al., 2007; Bishop and Pagiola, 2012;
41 Winsemius et al., 2013). Current watershed rehabilitation programs that focus on increasing
42 tree cover in upper watersheds are only partly aligned with current scientific evidence of effects
43 of large-scale tree planting on streamflow (Ghimire et al., 2014; Malmer et al., 2010; Palmer,
44 2009; van Noordwijk et al., 2007, 2015a; Verbist et al., 2010). The relationship between floods
45 and change in forest quality and quantity, and the availability of evidence for such a relationship
46 at various scales has been widely discussed over the past decades (Andréassian, 2004;
47 Bruijnzeel, 2004; Bradshaw et al., 2007; van Dijk et al., 2009). Measurements in Cote d'Ivoire,
48 for example, showed strong scale dependence of runoff from 30-50% at 1 m² point scale, to 4%
49 at 130 ha watershed scale, linked to spatial variability of soil properties plus variations in
50 rainfall patterns (Van de Giesen et al., 2000). The ratio between peak and average flow
51 decreases from headwater streams to main rivers in a predictable manner; while mean annual
52 discharge scales with (area)^{1.0}, maximum river flow was found to scale with (area)^{0.7} on average
53 (Rodríguez-Iturbe and Rinaldo, 2001; van Noordwijk et al., 1998). The determinants of peak
54 flow are thus scale-dependent, with space-time correlations in rainfall interacting with
55 subcatchment-level flow buffering at any point along the river. Whether and where peak flows
56 lead to flooding depends on the capacity of the rivers to pass on peak flows towards downstream
57 lakes or the sea, assisted by riparian buffer areas with sufficient storage capacity (Baldasarre et
58 al., 2013); reducing local flooding risk by increased drainage increases flooding risk
59 downstream, challenging the nested-scales management of watersheds to find an optimal spatial
60 distribution, rather than minimization, of flooding probabilities. Well-studied effects of forest
61 conversion on peak flows in small upper stream catchments (Alila et al., 2009) do not
62 necessarily translate to flooding downstream. As summarized by Beck et al. (2013) meso- to
63 macroscale catchment studies (>1 and >10 000 km², respectively) in the tropics, subtropics, and
64 warm temperate regions have mostly failed to demonstrate a clear relationship between river
65 flow and change in forest area. Lack of evidence cannot be firmly interpreted as evidence for
66 lack of effect, however. Detectability of effects depends on their relative size, the accuracy of
67 the measurement devices, background variability of the signal and length of observation period.
68 A recent econometric study for Peninsular Malaysia by Tan-Soo et al. (2014) concluded that,
69 after appropriate corrections for space-time correlates in the data-set for 31 meso- and
70 macroscale basins (554-28,643 km²), conversion of inland rain forest to monocultural

71 plantations of oil palm or rubber increased the number of flooding days reported, but not the
72 number of flood events, while conversion of wetland forests to urban areas reduced downstream
73 flood duration. This Malaysian study may be the first credible empirical evidence at this scale.
74 The difference between results for flood duration and flood frequency and the result for draining
75 wetland forests warrant further scrutiny. Consistency of these findings with river flow models
76 based on a water balance and likely pathways of water under the influence of change in land
77 cover and land use has yet to be shown. Two recent studies for Southern China confirm the
78 conventional perspective that deforestation increases high flows, but are contrasting in effects
79 of reforestation. Zhou et al. (2010) analysed a 50-year data set for Guangdong Province in China
80 and concluded that forest recovery had not changed the annual water yield (or its underpinning
81 water balance terms precipitation and evapotranspiration), but had a statistically significant
82 positive effect on dry season (low) flows. Liu et al. (2015), however, found for the Meijiang
83 watershed (6983 km²) in subtropical China that while historical deforestation had decreased
84 the magnitudes of low flows (daily flows \leq Q95%) by 30.1%, low flows were not significantly
85 improved by reforestation. They concluded that recovery of low flows by reforestation may
86 take much longer time than expected probably because of severe soil erosion and resultant loss
87 of soil infiltration capacity after deforestation. Changes in river flow patterns over a limited
88 period of time can be the combined and interactive effects of variations in the local rainfall
89 regime, land cover effects on soil structure and engineering modifications of water flow, that
90 can be teased apart with modelling tools (Ma et al., 2014).

91 Lacombe et al. (2015) documented that the hydrological effects of natural regeneration differ
92 from those of plantation forestry, while forest statistics do not normally differentiate between
93 these different land covers. In a regression study of the high and low flow regimes in the Volta
94 and Mekong river basins Lacombe and McCartney (2016) found that in the variation among
95 tributaries various aspects of land cover and land cover change had explanatory power. Between
96 the two basins, however, these aspects differed. In the Mekong basin variation in forest cover
97 had no direct effect on flows, but extending paddy areas resulted in a decrease in downstream
98 low flows, probably by increasing evapotranspiration in the dry season. In the Volta River
99 Basin, the conversion of forests to crops (or a reduction of tree cover in the existing parkland
100 system) induced greater downstream flood flows. This observation is aligned with the
101 experimental identification of an optimal, intermediate tree cover from the perspective of
102 groundwater recharge in parklands in Burkina Faso (Ilstedt et al., 2016).

103 The statistical challenges of attribution of cause and effect in such data-sets are considerable
104 with land use/land cover interacting with spatially and temporally variable rainfall, geological
105 configuration and the fact that land use is not changing in random fashion or following any pre-
106 randomized design (Alila et al., 2009; Rudel et al., 2005). Hydrological analysis across 12
107 catchments in Puerto Rico by Beck et al. (2013) did not find significant relationships between
108 the change in forest cover or urban area, and change in various flow characteristics, despite
109 indications that regrowing forests increased evapotranspiration. Yet, the concept of a
110 ‘regulating function’ on river flow regime for forests and other semi-natural ecosystems is
111 widespread. The considerable human and economic costs of flooding at locations and times
112 beyond where this is expected make the presumed ‘regulating function’ on flood reduction of
113 high value (Brauman et al., 2007) – if only we could be sure that the effect is real, beyond the
114 local scales ($< 10 \text{ km}^2$) of paired catchments where ample direct empirical proof exists
115 (Bruijnzeel, 1990, 2004). These observations imply that percent tree cover (or other forest
116 related indicators) is probably not a good metric for judging the ecosystem services provided
117 by a watershed (of different levels of ‘health’), and that a metric more directly reflecting
118 changes in river flow may be needed. Here we will explore a simple recursive model of river
119 flow (van Noordwijk et al., 2011) that (i) is focused on (loss of) predictability, (ii) can account
120 for the types of results obtained by the cited recent Malaysian study (Tan-Soo et al., 2014), and
121 (iii) may constitute a suitable performance indicator to monitor watershed ‘health’ through time.

122 \Rightarrow Figure 1

123 Figure 1 is compatible with a common dissection of risk as the product of hazard, exposure and
124 vulnerability. Extreme discharge events plus river-level engineering co-determine hazard, while
125 exposure depends on topographic position interacting with human presence, and vulnerability
126 can be modified by engineering at a finer scale and be further reduced by advice to leave an
127 area in high-risk periods. A recent study (Jongman et al., 2015) found that human fatalities and
128 material losses between 1980 and 2010 expressed as a share of the exposed population and
129 gross domestic product were decreasing with rising income. The planning needed to avoid
130 extensive damage requires quantification of the risk of higher than usual discharges, especially
131 at the upper tail end of the flow frequency distribution.

132 The statistical scarcity, per definition, of ‘extreme events’ and the challenge of data collection
133 where they do occur, make it hard to rely on empirical data as such. Existing data on flood
134 frequency and duration, as well as human and economic damage are influenced by topography,
135 human population density and economic activity, interacting with engineered infrastructure

136 (step 4 and 5 in Figure 1), as well as the extreme rainfall events that are their proximate cause.
137 Subsidence due to groundwater extraction in urban areas of high population density is a specific
138 problem for a number of cities built on floodplains (such as Jakarta and Bangkok), but
139 subsidence of drained peat areas has also been found to increase flooding risks elsewhere
140 (Sumarga et al., 2016). Common hydrological analysis of flood frequency (called 1 in 10-, 1 in
141 100-, 1 in 1000-year flood events, for example) does not separately attribute flood magnitude
142 to rainfall and land use properties, and analysis of likely change in flood frequencies in the
143 context of climate change adaptation has been challenging (Milly et al., 2002; Ma et al., 2014).
144 There is a lack of simple performance indicators for watershed health at its point of relating
145 precipitation P and river flow Q (step 2 in Figure 1) that align with local observations of river
146 behaviour and concerns about its change and that can reconcile local, public/policy and
147 scientific knowledge, thereby helping negotiated change in watershed management (Leimona
148 et al., 2015). The behaviour of rivers depends on many climatic (step 1 in Figure 1) and terrain
149 factors (step 7-9 in Figure 1) that make it a challenge to differentiate between anthropogenically
150 induced ecosystem structural change and soil degradation (step 7a) on one hand and intrinsic
151 variability on the other. Arrow 10 in Figure 1 represents the direct influence of climate on
152 vegetation, but also a possible reverse influence (van Noordwijk et al., 2015b). Hydrological
153 models tend to focus on predicting hydrographs at one or more temporal scales, and are usually
154 tested on data-sets from limited locations. Despite many decades (if not centuries) of
155 hydrological modelling, current hydrologic theory, models and empirical methods have been
156 found to be largely inadequate for sound predictions in ungauged basins (Hrachowitz et al.,
157 2013). Efforts to resolve this through harmonization of modelling strategies have so far failed.
158 Existing models differ in the number of explanatory variables and parameters they use, but are
159 generally dependent on empirical data of rainfall that are available for specific measurement
160 points but not at the spatial resolution that is required for a close match between measured and
161 modelled river flow. Spatially explicit models have conceptual appeal (Ma et al., 2010) but
162 have too many degrees of freedom and too many opportunities for getting right answers for
163 wrong reasons if used for empirical calibration (Beven, 2011). Parsimonious, parameter-sparse
164 models are appropriate for the level of evidence available to constrain them, but these
165 parameters are themselves implicitly influenced by many aspects of existing and changing
166 features of the watershed, making it hard to use such models for scenario studies of interacting
167 land use and climate change. Here we present a more direct approach deriving a metric of flow

168 predictability that can bridge local concerns and concepts to quantified hydrologic function: the
169 ‘flow persistence’ parameter (step 2 in Figure 1).

170 In this contribution to the debate we will first define the metric ‘flow persistence’ in the context
171 of temporal autocorrelation of river flow and then derive a way to estimate its numerical value.

172 In part II we will apply the algorithm to river flow data for a number of contrasting meso-scale
173 watersheds. In the discussion of this paper we will consider the new flow persistence metric in
174 terms of three groups of criteria for usable knowledge (Clark et al., 2011; Lusiana et al., 2011;
175 Leimona et al., 2015) based on salience (1,2), credibility (3,4) and legitimacy (5-7):

176 1. Does flow persistence relate to important aspects of watershed behaviour?

177 2. Does its quantification help to select management actions?

178 3. Is there consistency of numerical results?

179 4. How sensitive is it to bias and random error in data sources?

180 5. Does it match local knowledge?

181 6. Can it be used to empower local stakeholders of watershed management?

182 7. Can it inform local risk management?

183 Questions 3 and 4 will get specific attention in part II.

184 **2 Recursive river flow model and flow persistence**

185 **2.1 Basic equations**

186 One of the easiest-to-observe aspects of a river is its day-to-day fluctuation in water level,
187 related to the volumetric flow (discharge) via rating curves (Maidment, 1992). Without
188 knowing details of upstream rainfall and the pathways the rain takes to reach the river,
189 observation of the daily fluctuations in water level allows important inferences to be made. It
190 is also of direct utility: sudden rises can lead to floods without sufficient warning, while rapid
191 decline makes water utilization difficult. Indeed, a common local description of watershed
192 degradation is that rivers become more ‘flashy’ and less predictable, having lost a buffer or
193 ‘sponge’ effect (Joshi et al., 2004; Ranieri et al., 2004; Rahayu et al., 2013). A simple model of
194 river flow at time t , Q_t , is that it is similar to that of the day before (Q_{t-1}), to the degree F_p , a

195 dimensionless parameter called ‘flow persistence’ (van Noordwijk et al., 2011) plus an
196 additional stochastic term $Q_{a,t}$:

197 $Q_t = F_p Q_{t-1} + Q_{a,t}$ [1].

198 Q_t is for this analysis expressed in mm d^{-1} , which means that measurements in $\text{m}^3 \text{s}^{-1}$ need to be
199 divided by the relevant catchment area, with appropriate unit conversion. If river flow were
200 constant, it would be perfectly predictable, i.e. F_p would be 1.0 and $Q_{a,t}$ zero; in contrast, an F_p -
201 value equal to zero and $Q_{a,t}$ directly reflecting erratic rainfall represents the lowest possible
202 level of predictability.

203 The F_p parameter is conceptually identical to the ‘recession constant’ commonly used in
204 hydrological models, typically assessed during an extended dry period when the $Q_{a,t}$ term is
205 negligible and streamflow consists of base flow only (Tallaksen, 1995); empirical deviations
206 from a straight line in a plot of the logarithm of Q against time are common and point to multiple
207 rather than a single groundwater pool that contributes to base flow. The larger catchment area
208 has a possibility to get additional flow from multiple independent groundwater contribution.

209 As we will demonstrate in a next section, it is possible to derive F_p even when $Q_{a,t}$ is not
210 negligible. In climates without distinct dry season this is essential; elsewhere it allows a
211 comparison of apparent F_p between wet and dry parts of the hydrologic year. A possible
212 interpretation, to be further explored, is that decrease over the years of F_p indicates ‘watershed
213 degradation’ (i.e. greater contrast between high and low flows), and an increase ‘improvement’
214 or ‘rehabilitation’ (i.e. more stable flows).

215 If we consider the sum of river flow over a period of time (from 1 to T) we obtain

216 $\sum_1^T Q_t = F_p \sum_1^T Q_{t-1} + \sum_1^T Q_{a,t}$ [2].

217 If the period is sufficiently long period for Q_T minus Q_0 (the values of Q_t for $t=T$ and $t=0$,
218 respectively) to be negligibly small relative to the sum over all t ’s, we may equate $\sum_1^T Q_t$ with
219 $\sum_1^T Q_{t-1}$ and obtain a first way of estimating the F_p value:

220 $F_p = 1 - \sum_1^T Q_{a,t} / \sum_1^T Q_t$ [3].

221 Rearranging Eq.(3) we obtain

222 $\sum_1^T Q_{a,t} = (1 - F_p) \sum_1^T Q_t$ [4].

223 The $\sum Q_{a,t}$ term reflects the sum of peak flows in mm, while $F_p \sum Q_t$ reflects the sum of base
224 flow, also in mm. Clarifying the Q_a contribution is equivalent with one of several ways to

225 separate base flow from peak flows. For $F_p = 1$ (the theoretical maximum) we conclude that all
226 $Q_{a,t}$ must be zero, and all flow is ‘base flow’.

227 The stochastic $Q_{a,t}$ can be interpreted in terms of what hydrologists call ‘effective rainfall’ (i.e.
228 rainfall minus on-site evapotranspiration, assessed over a preceding time period t_x since
229 previous rain event):

230 $Q_t = F_p Q_{t-1} + (1-F_p)(P_{tx} - E_{tx})$ [5].

231 Where P_{tx} is the (spatially weighted) precipitation (assuming no snow or ice, which would shift
232 the focus to snowmelt) in mm d^{-1} ; E_{tx} , also in mm d^{-1} , is the preceding evapotranspiration that
233 allowed for infiltration during this rainfall event (*i.e.* evapotranspiration since the previous soil-
234 replenishing rainfall that induced empty pore space in the soil for infiltration and retention), or
235 replenishment of a waterfilm on aboveground biomass that will subsequently evaporate. More
236 complex attributions are possible, aligning with the groundwater replenishing bypass flow and
237 the water isotopic fractionation involved in evaporation (Evaristo et al., 2015).

238 The consistency of multiplying effective rainfall with $(1-F_p)$ can be checked by considering the
239 geometric series $(1-F_p)$, $(1-F_p) F_p$, $(1-F_p) F_p^2$, ..., $(1-F_p) F_p^n$ which adds up to $(1-F_p)(1 - F_p^n)/(1 -$
240 $F_p)$ or $1 - F_p^n$. This approaches 1 for large n , suggesting that all of the water attributed to time
241 t , *i.e.* $P_t - E_{tx}$, will eventually emerge as river flow. For $F_p = 0$ all of $(P_t - E_{tx})$ emerges on the
242 first day, and river flow is as unpredictable as precipitation itself. For $F_p = 1$ all of $(P_t - E_{tx})$
243 contributes to the stable daily flow rate, and it takes an infinitely long period of time for the last
244 drop of water to get to the river. For declining F_p , $(1 > F_p > 0)$, river flow gradually becomes
245 less predictable, because a greater part of the stochastic precipitation term contributes to
246 variable rather than evened-out river flow.

247 Taking long term summations of the right- and left- hand sides of Eq.(5) we obtain:

248 $\Sigma Q_t = \Sigma (F_p Q_{t-1} + (1-F_p)(P_t - E_{tx})) = F_p \Sigma Q_{t-1} + (1-F_p)(\Sigma P_t - \Sigma E_{tx})$ [6].

249 Which is consistent with the basic water budget, $\Sigma Q = \Sigma P - \Sigma E$, at time scales long enough for
250 changes in soil water buffer stocks to be ignored. As such the total annual, and hence the mean
251 daily river flow are independent of F_p . This does not preclude that processes of watershed
252 degradation or restoration that affect the partitioning of P over Q and E also affect F_p .

253 **2.2 Low flows**

254 The lowest flow expected in an annual cycle is $Q_x F_p^{N_{max}}$ where Q_x is flow on the first day
255 without rain and N_{max} the longest series of dry days. Taken at face value, a decrease in F_p has
256 a strong effect on low-flows, with a flow of 10% of Q_x reached after 45, 22, 14, 10, 8 and 6
257 days for $F_p = 0.95, 0.9, 0.85, 0.8, 0.75$ and 0.7, respectively. However, the groundwater
258 reservoir that is drained, equalling the cumulative dry season flow if the dry period is
259 sufficiently long, is $Q_x/(1-F_p)$. If F_p decreases to F_{px} but the groundwater reservoir ($Res =$
260 $Q_x/(1-F_p)$) is not affected, initial flows in the dry period will be higher ($Q_x F_{px}^i (1-F_{px}) Res >$
261 $Q_x F_p^i (1-F_p) Res$ for $i < \log((1-F_{px})/(1-F_p))/\log(F_p/F_{px})$). It thus matters how low flows are
262 evaluated: from the perspective of the lowest level reached, or as cumulative flow. The
263 combination of climate, geology and land form are the primary determinants of cumulative
264 low flows, but if land cover reduces the recharge of groundwater there may be impacts on dry
265 season flow, that are not directly reflected in F_p .

266 If a single F_p value would account for both dry and wet season, the effects of changing F_p on
267 low flows may well be more pronounced than those on flood risk. Empirical tests are needed
268 of the dependence of F_p on Q (see below). Analysis of the way an aggregate F_p depends on
269 the dominant flow pathways provides a basis for differentiating F_p within a hydrologic year.

271 **2.3 Flow-pathway dependence of flow persistence**

272 The patch-level partitioning of water between infiltration and overland flow is further modified
273 at hillslope level, with a common distinction between three pathways that reach streams:
274 overland flow, interflow and groundwater flow (Band et al., 1993; Weiler and McDonnell,
275 2004). An additional interpretation of Eq.(1), potentially adding to our understanding of results
276 but not needed for analysis of empirical data, can be that three pathways of water through a
277 landscape contribute to river flow (Barnes, 1939): groundwater release with $F_{p,g}$ values close to
278 1.0, overland flow with $F_{p,o}$ values close to 0, and interflow with intermediate $F_{p,i}$ values.

279 $Q_t = F_{p,g} Q_{t-1,g} + F_{p,i} Q_{t-1,i} + F_{p,o} Q_{t-1,o} + Q_{a,t}$ [7],

280 $F_p = (F_{p,g} Q_{t-1,g} + F_{p,i} Q_{t-1,i} + F_{p,o} Q_{t-1,o})/Q_{t-1}$ [8].

281 On this basis a decline or increase in overall weighted average F_p can be interpreted as indicator
282 of a shift of dominant runoff pathways through time within the watershed. Dry season flows
283 are dominated by $F_{p,g}$. The effective F_p in the rainy season can be interpreted as indicating the

284 relative importance of the other two flow pathways. F_p reflects the fractions of total river flow
285 that are based on groundwater, overland flow and interflow pathways:

286
$$F_p = F_{p,g} (\Sigma Q_{t,g} / \Sigma Q_t) + F_{p,o} (\Sigma Q_{t,o} / \Sigma Q_t) + F_{p,i} (\Sigma Q_{t,i} / \Sigma Q_t) \quad [9].$$

287 Beyond the type of degradation of the watershed that, mostly through soil compaction, leads to
288 enhanced infiltration-excess (or Hortonian) overland flow (Delfs et al., 2009), saturated
289 conditions throughout the soil profile may also induce overland flow, especially near valley
290 bottoms (Bonell, 1993; Bruijnzeel, 2004). Thus, the value of $F_{p,o}$ can be substantially above
291 zero if the rainfall has a significant temporal autocorrelation, with heavy rainfall on subsequent
292 days being more likely than would be expected from general rainfall frequencies. If rainfall
293 following a wet day is more likely to occur than following a dry day, as is commonly observed
294 in Markov chain analysis of rainfall patterns (Jones and Thornton, 1997; Bardossy and Plate,
295 1991), the overland flow component of total flow will also have a partial temporal
296 autocorrelation, adding to the overall predictability of river flow. In a hypothetical climate with
297 evenly distributed rainfall, we can expect F_p to be 1.0 even if there is no infiltration and the only
298 pathway available is overland flow. Even with rainfall that is variable at any point of
299 observation but has low spatial correlation it is possible to obtain F_p values of (close to) 1.0 in
300 a situation with (mostly) overland flow (Ranieri et al., 2004).

301 **3. Methods**

302 **3.1 Numerical example**

303 Figure 2 provides an example of the way a change in F_p values (based on Eq. 1) influences the
304 pattern of river flow for a unimodal rainfall regime with a well-developed dry season. The figure
305 was constructed in a Monte Carlo realization of rainfall based on a (truncated) sinus-based
306 probability of rainfall and rectangular rainfall depth to derive the $(P_{tx} - E_{tx})$ term, with the $Q_{a,t}$
307 values derived as $(1 - F_p) (P_{tx} - E_{tx})$. The increasing ‘spikiness’ of the graph as F_p is lowered
308 indicates reduced predictability of flow on any given day during the wet season on the basis of
309 the flow on the preceding day. A bi-plot of river flow on subsequent days for the same
310 simulations (Figure 3) shows two main effects of reducing the F_p value: the scatter increases,
311 and the slope of the lower envelope containing the swarm of points is lowered (as it equals F_p).
312 Both of these changes can provide entry points for an algorithm to estimate F_p from empirical
313 time series, provided the basic assumptions of the simple model apply and the data are of

314 acceptable quality (see Section 3 below). For the numerical example shown in Figure 2, the
315 maximum daily flow doubled from 50 to 100 mm when the F_p value decreased from a value
316 close to 1 (0.98) to nearly 0.

317 \Rightarrow Figure 2
318 \Rightarrow Figure 3

319 **3.2 Flow persistence as a simple flood risk indicator**

320 For numerical examples (implemented in a spreadsheet model) flow on each day can be derived
321 as:

322 $Q_t = \sum_j F_p^{t-j} (1-F_p) p_j P_j$ [10].

323 Where p_j reflects the occurrence of rain on day j (reflecting a truncated sine distribution for
324 seasonal trends) and P_j is the rain depth (drawn from a uniform distribution). From this model
325 the effects of F_p (and hence of changes in F_p) on maximum daily flow rates, plus maximum
326 flow totals assessed over a 2-5 d period, was obtained in a Monte Carlo process (without
327 Markov autocorrelation of rainfall in the default case – see below). Relative flood protection
328 was calculated as the difference between peak flows (assessed for 1-5 d duration after a 1 year
329 ‘warm-up’ period) for a given F_p versus those for $F_p = 0$, relative to those at $F_p = 0$.

330 **3.3 An algorithm for deriving F_p from a time series of stream flow data**

331 Equation (3) provides a first method to derive F_p from empirical data if these cover a full
332 hydrologic year. In situations where there is no complete hydrograph and/or in situations where
333 we want to quantify F_p for shorter time periods (e.g. to characterise intraseasonal flow patterns)
334 and the change in the storage term of the water budget equation cannot be ignored, we need an
335 algorithm for estimating F_p from a series of daily Q_t observations.

336 Where rainfall has clear seasonality, it is attractive and indeed common practice to derive a
337 groundwater recession rate from a semi-logarithmic plot of Q against time (Tallaksen, 1995).
338 As we can assume for such periods that $Q_{a,t} = 0$, we obtain $F_p = Q_t / Q_{t-1}$, under these
339 circumstances. We cannot be sure, however, that this $F_{p,g}$ estimate also applies in the rainy
340 season, because overall wet-season F_p will include contributions by $F_{p,o}$ and $F_{p,i}$ as well
341 (compare Eq. 9). In locations without a distinct dry season, we need an alternative method.

342 A biplot of Q_t against Q_{t-1} (as in Figure 3) will lead to a scatter of points above a line with slope
343 F_p , with points above the line reflecting the contributions of $Q_{a,t} > 0$, while the points that plot
344 on the F_p line itself represent $Q_{a,t} = 0 \text{ mm d}^{-1}$. There is no independent source of information on

345 the frequency at which $Q_{a,t} = 0$, nor what the statistical distribution of $Q_{a,t}$ values is if it is non-
346 zero. Calculating back from the Q_t series we can obtain an estimate ($Q_{a,Fptry}$) of $Q_{a,t}$ for any
347 given estimate ($F_{p,try}$) of F_p , and select the most plausible F_p value. For high $F_{p,try}$ estimates there
348 will be many negative $Q_{a,Fptry}$ values, for low $F_{p,try}$ estimates all $Q_{a,Fptry}$ values will be larger. An
349 algorithm to derive a plausible F_p estimate can thus make use of the corresponding distribution
350 of ‘apparent Q_a ’ values as estimates of $F_{p,try}$, calculated as $Q_{a,try} = Q_t - F_{p,try} Q_{t-1}$. While $Q_{a,t}$
351 cannot be negative in theory, small negative Q_a estimates are likely when using real-world data
352 with their inherent errors. The FlowPer F_p algorithm (van Noordwijk et al., 2011) derives the
353 distribution of $Q_{a,try}$ estimates for a range of $F_{p,try}$ values (Figure 4B) and selects the value $F_{p,try}$
354 that minimizes the variance $\text{Var}(Q_{a,Fptry})$ (or its standard deviation) (Figure 4C). It is
355 implemented in a spreadsheet workbook that can be downloaded from the ICRAF website
356 (<http://www.worldagroforestry.org/output/flowper-flow-persistence-model>)

357 → Figure 4

358 A consistency test is needed that the high-end Q_t values relate to Q_{t+1} in the same was as do low
359 or medium Q_t values. Visual inspection of Q_{t+1} versus Q_t , with the derived F_p value, provides a
360 qualitative view of the validity of this assumption. The F_p algorithm can be applied to any
361 population of (Q_{t-1}, Q_t) pairs, e.g. selected from a multiyear data set on the basis of 3-month
362 periods within the hydrological year.

363 4 Results

364 4.1 Flood intensity and duration

365 Figure 5 shows the effect of F_p values in the range 0 to 1 on the maximum flows obtained with
366 a random time series of ‘effective rainfall’, compared to results for $F_p = 0$. Maximum flows
367 were considered at time scales of 1 to 5 days, in a moving average routine. This way a relative
368 flood protection, expressed as reduction of peak flow, could be related to F_p (Figure 5A).

369 ⇒ Figure 5

370 Relative flood protection rapidly decreased from its theoretical value of 100% at $F_p = 1$ (when
371 there was no variation in river flow), to less than 10% at F_p values of around 0.5. Relative flood
372 protection was slightly lower when the assessment period was increased from 1 to 5 days
373 (between 1 and 3 d it decreased by 6.2%, from 3 to 5 d by a further 1.3%). Two counteracting
374 effects are at play here: a lower F_p means that a larger fraction ($1-F_p$) of the effective rainfall
375 contributes to river flow, but the increased flow is less persistent. In the example the flood

376 protection in situations where the rainfall during 1 or 2 d causes the peak is slightly stronger
377 than where the cumulative rainfall over 3-5 d causes floods, as typically occurs downstream.

378 As we expect from equation 5 that peak flow is to $(1-F_p)$ times peak rainfall amounts, the effect
379 of a change in F_p not only depends on the change in F_p that we are considering, but also on its
380 initial value. Higher initial F_p values will lead to more rapid increases in high flows for the same
381 reduction in F_p (Figure 5B). However, flood duration rather responds to changes in F_p in a
382 curvilinear manner, as flow persistence implies flood persistence (once flooding occurs), but
383 the greater the flow persistence the less likely such a flooding threshold is passed (Figure 5C).
384 The combined effect may be restricted to about 3 d of increase in flood duration for the
385 parameter values used in the default example, but for different parametrization of the stochastic
386 ε other results might be obtained.

387 **4.2 Algorithm for F_p estimates from river flow time series**

388 The algorithm has so far returned non-ambiguous F_p estimates on any modelled time series data
389 of river flow, as well as for all empirical data set we tested (including all examples tested in
390 part II), although there probably are data sets on which it can breakdown. Visual inspection of
391 Q_{t-1}/Q_t biplots (as in Figure 3) can provide clues to non-homogenous data sets, to potential
392 situations where effective F_p depends on flow level Q_t and where data are not consistent with a
393 straight-line lower envelope. Where river flow estimates were derived from a model with
394 random elements, however, variation in F_p estimates was observed, that suggests that specific
395 aspects of actual rainfall, beyond the basic characteristics of a watershed and its vegetation, do
396 have at least some effect. Such effects deserve to be further explored for a set of case studies,
397 as their strength probably depends on context.

398 **5 Discussion**

399 We will discuss the flow persistence metric based on the questions raised from the perspectives
400 of salience, credibility and legitimacy.

401 **5.1 Salience**

402 Key *salience* aspects are “Does flow persistence relate to important aspects of watershed
403 behaviour?” and “Does it help to select management actions?”. A major finding in the
404 derivation of F_p was that the flow persistence measured at daily time scale can be logically
405 linked to the long-term water balance, and that the proportion of peak rainfall that translates to

406 peak river flow equals the complement of flow persistence. This feature links effects on floods
407 of changes in watershed quality to effects on low flows, although not in a linear relationship.
408 The F_p parameter as such does not predict when and where flooding will occur, but it does help
409 to assess to what extent another condition of the watershed, with either higher or lower F_p would
410 translate the same rainfall into larger or small peak water flows. This is salient, especially if the
411 relative contributions of (anthropogenic) land cover and the (exogenous, probabilistic) specifics
412 of the rainfall pattern can be further teased apart (see part II). Where F_p may describe the
413 descending branch of hydrographs at a relevant time scale, details of the ascending branch
414 beyond the maximum daily flow reached may be relevant for reducing flood damage, and may
415 require more detailed study at higher temporal resolution.

416 A key strength of our flow persistence parameter, that it can be derived from observing river
417 flow at a single point along the river, without knowledge of rainfall events and catchment
418 conditions, is also its major weakness. If rainfall data exist, and especially rainfall data that
419 apply to each subcatchment, the Q_a term doesn't have to be treated as a random variable and
420 event-specific information on the flow pathways may be inferred for a more precise account of
421 the hydrograph. But for the vast majority of rivers in the tropics, advances in remotely sensed
422 rainfall data are needed to achieve that situation and F_p may be all that is available to inform
423 public debates on the relation between forests and floods.

424 Figures 2 and 5 show that most of the effects of a decreasing F_p value on peak discharge (which
425 is the basis for downstream flooding) occur between F_p values of 1 and 0.7, with the relative
426 flood protection value reduced to 10% when F_p reaches 0.5. As indicated in Figure 1, peak
427 discharge is only one of the factors contributing to flood risk in terms of human casualties and
428 physical damage. Flood risks are themselves nonlinearly and in strongly topography-specific
429 ways related to the volume of river flow after extreme rainfall events. While the expected
430 fraction of rainfall that contributes to direct flow is linearly related to rainfall via $(1-F_p)$,
431 flooding risk as such will have a non-linear relationship with rainfall, that depends on
432 topography and antecedent rainfall. Catchment changes, such as increases or decreases in
433 percentage tree cover, will generally have a non-linear relationship with F_p as well as with
434 flooding risks. The F_p value has an inverse effect on the fraction of recent rainfall that becomes
435 river flow, but the effect on peak flows is less, as higher F_p values imply higher base flow. The
436 way these counteracting effects balance out depends on details of the local rainfall pattern
437 (including its Markov chain temporal autocorrelation), as well as the downstream topography

438 and risk of people being at the wrong time at a given place, but the F_p value is an efficient way
439 of summarizing complex land use mosaics and upstream topography in its effect on river flow.
440 The difference between wet-season and dry-season F_p deserves further analysis. In climates
441 with a real rainless dry-season, dry season F_p is dominated by the groundwater release fraction
442 of the watershed, regardless of land cover, while in wet season it depends on the mix (weighted
443 average) of flow pathways. The degree to which F_p can be influenced by land cover needs to
444 be assessed for each landscape and land cover combination, including the locally relevant forest
445 and forest derived land classes, with their effects on interception, soil infiltration and time
446 pattern of transpiration. The F_p value can summarize results of models that explore land use
447 change scenarios in local context. To select the specific management actions that will maintain
448 or increase F_p a locally calibrated land use/hydrology model is needed, such as GenRiver (part
449 II), DHV (Bergström, 1995) or SWAT (Yen et al., 2015).

450 Although a higher F_p value will in most cases be desirable (and a decrease in F_p undesirable),
451 we may expect that downstream biota have adjusted to the pre-human flow conditions and its
452 inherent F_p and variability. Decreased variability of flow achieved by engineering interventions
453 (e.g. a reservoir with constant release of water to generate hydropower) may have negative
454 consequences for fish and other biota (Richter et al., 2003; McCluney et al., 2014).

455 The “health” concept we use is a comprehensive one of the way climate, watershed and
456 engineering interventions interact on functional aspects of river flow. In the catchments we
457 considered in part II there have been no major dams or reservoirs installed. Ma et al (2014)
458 described a method to separate these three influences on river flow. Where these do exist the
459 specific operating rules of reservoirs need to be included in any model and these can have a
460 major influence on downstream flow, depending on the primary use for power generation, dry
461 season irrigation or stabilizing river flow for riverine transport.

462 **5.2 Credibility**

463 Key *credibility* questions are “Consistency of numerical results?” and “How sensitive are
464 results to bias and random error in data sources?”. This is further discussed in part II, after a
465 number of case studies has been studied. The main conclusions are that intra-annual variability
466 of F_p values between wet and dry seasons was around 0.2 in the case studies, interannual
467 variability in either annual or seasonal F_p was generally in the 0.1 range, while the difference
468 between observed and simulated flow data as basis for F_p calculations was mostly less than 0.1.

469 With current methods, it seems that effects of land cover change on flow persistence that shift
470 the F_p value by about 0.1 are the limit of what can be asserted from empirical data (with shifts
471 of that order in a single year a warning sign rather than a firmly established change). When
472 derived from observed river flow data F_p is suitable for monitoring change (degradation,
473 restoration) and can be a serious candidate for monitoring performance in outcome-based
474 ecosystem service management contracts. In interpreting changes in F_p as caused by changes
475 in the condition in the watershed, however, changes in specific properties of the rainfall regime
476 must be excluded. At the scale of paired catchment studies this assumption may be reasonable,
477 but in temporal change (or using specific events as starting point for analysis), it is not easy to
478 disentangle interacting effects (Ma et al., 2014). Recent evidence that vegetation not only
479 responds to, but also influences rainfall (arrow 10 in Figure 1; van Noordwijk et al., 2015b)
480 further complicates the analysis across scales.

481 As indicated, the F_p method is related to earlier methods used in streamflow hydrograph
482 separation of base flow and quick flow. While textbooks (Ward and Robinson, 2000;
483 Hornberger et al 2014) tend to be critical of the lack of objectivity of graphical methods,
484 algorithms are used for deriving the minimum flow in a fixed or sliding period of reference as
485 base flow (Sloto and Crouse, 1996; Furey and Gupta, 2001). The time interval used for deriving
486 the minimum flow depends on catchment size. Figure 6 compares results for a hydrograph of a
487 single year of one of the catchments described in more detail in paper II. While there is
488 agreement on most of what is indicated as baseflow, the short term response to peaks in the
489 flow differ, with baseflow in the F_p method more rapidly increasing after peak events. When
490 compared across multiple years for the four catchments described in detail in paper II (figure
491 7), there is partial agreement in the way interannual variation is described in each catchment,
492 while numerical values are similar, but the ratio of what is indicated as baseflow according to
493 the F_p method and according to standard hydrograph separation varies from 1.05 to 0.86.

494 ⇒ Figure 6
495 ⇒ Figure 7

496 Recursive models that describe flow in a next time interval on the basis of a fraction of that in
497 the preceding time interval with a term for additional flow due to additional rainfall have been
498 used in analysis of peak flow event before, with time intervals as short as 1 minute rather than
499 the 1 day we use here (Rose, 2004). Through reference to an overall mass balance a relationship
500 similar to what we found here (F_p times preceding flow plus $1 - F_p$ times recent inputs) was

501 also used in such models. To our knowledge, the method we describe here at daily timescales
502 has not been used before.

503 The idea that the form of the storage-discharge function can be estimated from analysis of
504 streamflow fluctuations has been explored before for a class of catchments in which discharge
505 is determined by the volume of water in storage (Kirchner, 2009). Such catchments behave as
506 simple first-order nonlinear dynamical systems and can be characterized in a single-equation
507 rainfall-runoff model that predicted streamflow, in a test catchment in Wales, as accurately as
508 other models that are much more highly parameterized. This model of the dQ/dt versus Q
509 relationship can also be analytically inverted; thus, it can be used to “do hydrology backward,”
510 that is, to infer time series of whole-catchment precipitation directly from fluctuations in
511 streamflow. The slope of the log-log relationship between flow recession (dQ/dt) and Q that
512 Kirchner (2009) used is conceptually similar to the F_p metric we derived here, but the specific
513 algorithm to derive the parameter from empirical data differs. Estimates of dQ/dt are sensitive
514 to noise in the measurement of Q and the possibly frequent and small increases in Q can be
515 separated from the expected flow recession in the algorithm we presented here.

516 Seifert and Beven (2009) discussed the increase in predictive skill of models depending on the
517 amount of location-specific data that can be used to constrain them. They found that the
518 ensemble prediction of multiple models for a single location clearly outperformed the
519 predictions using single parameter sets and that surprisingly little runoff data was necessary to
520 identify model parameterizations that provided good results for “ungauged” test periods in
521 cases where actual measurements were available. Their results indicated that a few runoff
522 measurements can contain much of the information content of continuous runoff time series.
523 The way these conclusions might be modified if continuous measurements for limited time
524 periods, rather than separated single data points on river flow could be used, remains to be
525 explored. Their study indicated that results may differ significantly between catchments and
526 critical tests of F_p across multiple situations are obviously needed, as paper II will provide.

527 In discussions and models of temperate zone hydrology (Bergström, 1995; Seifert, 1999)
528 snowmelt is a major component of river flow and effects of forest cover on spring temperatures
529 are important to the buffering of the annual peaks in flow that tend to occur in this season.
530 Application of the F_p method to data describing such events has yet to be done.

531 **5.3 Legitimacy**

532 *Legitimacy* aspects are “Does it match local knowledge?” and “Can it be used to empower local
533 stakeholders of watershed management?” and “Can it inform risk management?”. As the F_p
534 parameter captures the predictability of river flow that is a key aspect of degradation according
535 to local knowledge systems, its results are much easier to convey than full hydrographs or
536 exceedance probabilities of flood levels. By focusing on observable effects at river level, rather
537 than prescriptive recipes for land cover (“reforestation”), the F_p parameter can be used to more
538 effectively compare the combined effects of land cover change, changes in the riparian wetlands
539 and engineered water storage reservoirs, in their effect on flow buffering. It is a candidate for
540 shifting environmental service reward contracts from input to outcome based monitoring (van
541 Noordwijk et al., 2012). As such it can be used as part of a negotiation support approach to
542 natural resources management in which levelling off on knowledge and joint fact finding in
543 blame attribution are key steps to negotiated solutions that are legitimate and seen to be so (van
544 Noordwijk et al., 2013; Leimona et al., 2015). Quantification of F_p can help assess tactical
545 management options (Burt et al., 2014) as in a recent suggestion to minimize negative
546 downstream impacts of forestry operations on stream flow by avoiding land clearing and
547 planting operations in locally wet La Niña years. But the most challenging aspect of the
548 management of flood, as any other environmental risk, is that the frequency of disasters is too
549 low to intuitively influence human behaviour where short-term risk taking benefits are
550 attractive. Wider social pressure is needed for investment in watershed health (as a type of
551 insurance premium) to be mainstreamed, as individuals waiting to see evidence of necessity are
552 too late to respond. In terms of flooding risk, actions to restore or retain watershed health can
553 be similarly justified as insurance premium. It remains to be seen whether or not the
554 transparency of the F_p metric and its intuitive appeal are sufficient to make the case in public
555 debate when opportunity costs of foregoing reductions in flow buffering by profitable land use
556 are to be compensated and shared (Burt et al., 2014).

557 **5.4 Conclusions and specific questions for a set of case studies**

558 In conclusion, the F_p metric appears to allow an efficient way of summarizing complex
559 landscape processes into a single parameter that reflects the effects of landscape management
560 within the context of the local climate. If rainfall patterns change but the landscape does not,
561 the resultant flow patterns may reflect a change in watershed health (van Noordwijk et al.,
562 2016). Flow persistence is the result of rainfall persistence and the temporal delay provided by

563 the pathway water takes through the soil and the river system. High flow persistence indicates
564 a reliable water supply, while minimizing peak flow events. Wider tests of the F_p metric as
565 boundary object in science-practice-policy boundary chains (Kirchhoff et al., 2015; Leimona et
566 al., 2015) are needed. Further tests for specific case studies can clarify how changes in tree
567 cover (deforestation, reforestation, agroforestation) in different contexts influence river flow
568 dynamics and F_p values. Sensitivity to specific realizations of underlying time-space rainfall
569 patterns needs to be quantified, before changes in F_p can be attributed to ‘watershed quality’,
570 rather than chance events.

571 **Data availability**

572 The algorithm used is freely available. Specific data used in the case studies are explained and
573 accounted for in Part II.

574 **Author contributions**

575 Meine van Noordwijk designed method and paper, Lisa Tanika refined the empirical algorithm
576 and handled the case study data and modelling for part II, and Betha Lusiana contributed
577 statistical analysis; all contributed and approved the final manuscript

578 **Acknowledgements**

579 This research is part of the Forests, Trees and Agroforestry research program of the CGIAR.
580 Several colleagues contributed to the development and early tests of the F_p method. Thanks are
581 due to Eike Luedeling, Sonya Dewi, Sampurno Bruijnzeel and two anonymous reviewers for
582 comments on an earlier version of the manuscript.

583 **References**

584 Alila, Y., Kura, P.K., Schnorbus, M., and Hudson, R.: Forests and floods: A new paradigm
585 sheds light on age-old controversies, *Water Resour. Res.*, 45, W08416, 2009.

586 Andréassian, V.: Waters and forests: from historical controversy to scientific debate, *Journal of
587 Hydrology*, 291, 1–27, 2004.

588 Baldassarre, G.D., Kooy, M., Kemerink, J.S., and Brandimarte, L.: Towards understanding the
589 dynamic behaviour of floodplains as human-water systems, *Hydrology and Earth System
590 Sciences*, 17(8), 3235–3244, 2013.

591 Bardossy, A. and Plate, E.J.: Modeling daily rainfall using a semi-Markov representation of
592 circulation pattern occurrence, *Journal of Hydrology*, 122(1), 33-47, 1991.

593 Band, L.E., Patterson, P., Nemani, R., and Running, S.W.: Forest ecosystem processes at the
594 watershed scale: incorporating hillslope hydrology, *Agricultural and Forest Meteorology*,
595 63(1-2), 93-126, 1993.

596 Barnes, B.S.: The structure of discharge-recession curves, *Eos, Transactions American
597 Geophysical Union*, 20(4), 721-725, 1939.

598 Beck, H. E., Bruijnzeel, L. A., Van Dijk, A. I. J. M., McVicar, T. R., Scatena, F. N., and
599 Schellekens, J.: The impact of forest regeneration on streamflow in 12 mesoscale humid
600 tropical catchments, *Hydrology and Earth System Sciences*, 17(7), 2613-2635, 2013.

601 Bergström, S.: The HBV model. In: Singh, V.P., (Ed.), *Computer Models of Watershed
602 Hydrology*, Ch. 13, pp. 443-476, Water Resources Publications, Highlands Ranch,
603 Colorado, USA, 1130 pp., 1995.

604 Beven, K.J.: Rainfall-runoff modelling: the primer, John Wiley & Sons, 2011

605 Bishop, J. and Pagiola, S. (Eds.): *Selling forest environmental services: market-based
606 mechanisms for conservation and development*, Taylor & Francis, Abingdon (UK), 2012.

607 Bonell, M.: Progress in the understanding of runoff generation dynamics in forests, *Journal of
608 Hydrology*, 150(2), 217-275, 1993.

609 Bradshaw, C.J.A., Sodhi, N.S., Peh, K.S.H., and Brook, B.W.: Global evidence that
610 deforestation amplifies flood risk and severity in the developing world, *Global Change Biol.*,
611 13, 2379–2395, 2007.

612 Brauman, K.A., Daily, G.C., Duarte, T.K.E., and Mooney, H.A.: The nature and value of
613 ecosystem services: an overview highlighting hydrologic services, *Annu. Rev. Environ.
614 Resour.*, 32, 67-98, 2007.

615 Bruijnzeel, L.A.: Hydrological functions of tropical forests: not seeing the soil for the trees,
616 *Agr. Ecosyst. Environ.*, 104, 185–228, 2004.

617 Burt, T.P., Howden, N.J.K., McDonnell, J.J., Jones, J.A., and Hancock, G.R.: Seeing the
618 climate through the trees: observing climate and forestry impacts on streamflow using a 60-
619 year record, *Hydrological Processes*, doi: 10.1002/hyp.10406, 2014.

620 Clark, W. C., Tomich, T. P., van Noordwijk, M., Guston, D., Catacutan, D., Dickson, N. M.,
621 and McNie, E.: Boundary work for sustainable development: natural resource management
622 at the Consultative Group on International Agricultural Research (CGIAR), Proc. Nat.
623 Acad. Sci., doi:10.1073/pnas.0900231108, 2011.

624 Delfs, J.O., Park, C.H., and Kolditz, O.: A sensitivity analysis of Hortonian flow, Advances in
625 Water Resources. 32(9), 1386-1395, 2009.

626 Evaristo, J., Jasechko, S., and McDonnell, J.J.: Global separation of plant transpiration from
627 groundwater and streamflow, Nature, 525(7567), 91-94, 2015.

628 Furey, P.R. and Gupta, V.K.: A physically based filter for separating base flow from streamflow
629 time series. *Water Resources Research*, 37(11), 2709-2722, 2001.

630 Ghimire, C.P., Bruijnzeel, L.A., Lubczynski, M.W., and Bonell, M.: Negative trade-off
631 between changes in vegetation water use and infiltration recovery after reforesting degraded
632 pasture land in the Nepalese Lesser Himalaya, *Hydrology and Earth System
633 Sciences*, 18(12), 4933-4949, 2014.

634 Hornberger, G.M., Wiberg, P.L., D'Odorico, P. and Raffensperger, J.P.: *Elements of physical
635 hydrology*. John Hopkins Univesity Press, 2014.

636 Hrachowitz, M., Savenije, H.H.G., Blöschl, G., McDonnell, J.J., Sivapalan, M., Pomeroy, J.W.,
637 Arheimer, B., Blume, T., Clark, M. P., Ehret, U., Fenicia, F., Freer, J E., Gelfan, A., Gupta,
638 H.V., Hughes, D. A., Hut, R.W., Montanari, A., Pande, S., Tetzlaff, D., Troch, P.A.,
639 Uhlenbrook, S., Wagener, T., Winsemius, H.C., Woods, R.A., Zehe, E., and Cudennec, C.:
640 A decade of Predictions in Ungauged Basins (PUB)—a review, *Hydrological sciences
641 journal*, 58(6), 1198-1255, 2013.

642 Ilstedt, U., Tobella, A.B., Bazié, H.R., Bayala, J., Verbeeten, E., Nyberg, G., Sanou, J.,
643 Benegas, L., Murdiyarso, D., Laudon, H., and Sheil, D.: Intermediate tree cover can
644 maximize groundwater recharge in the seasonally dry tropics, *Scientific reports*, 6, 2016

645 Jones, P.G. and Thornton, P.K.: Spatial and temporal variability of rainfall related to a third-
646 order Markov model, *Agricultural and Forest Meteorology*, 86(1), 127-138, 1997.

647 Jongman, B., Winsemius, H. C., Aerts, J. C., de Perez, E. C., van Aalst, M. K., Kron, W., and
648 Ward, P. J.: Declining vulnerability to river floods and the global benefits of adaptation, In:
649 *Proceedings of the National Academy of Sciences*, 112(18), E2271-E2280, 2015.

650 Joshi, L., Schalenbourg, W., Johansson, L., Khasanah, N., Stefanus, E., Fagerström, M.H., and
651 van Noordwijk, M.: Soil and water movement: combining local ecological knowledge with
652 that of modellers when scaling up from plot to landscape level, In: van Noordwijk, M.,
653 Cadisch, G. and Ong, C.K. (Eds.) Belowground Interactions in Tropical Agroecosystems,
654 CAB International, Wallingford (UK), 349-364, 2004.

655 Kirchhoff, C.J., Esselman, R., and Brown, D.: Boundary Organizations to Boundary Chains:
656 Prospects for Advancing Climate Science Application, Climate Risk Management,
657 doi:10.1016/j.crm.2015.04.001, 2015.

658 Kirchner, J.W.: Catchments as simple dynamical systems: Catchment characterization, rainfall-
659 runoff modeling, and doing hydrology backward. *Water Resources Research*, 45(2).
660 DOI: 10.1029/2008WR006912, 2009.

661 Lacombe, G. and McCartney, M.: Evaluating the flow regulating effects of ecosystems in the
662 Mekong and Volta river basins, Colombo, Sri Lanka, International Water Management
663 Institute (IWMI) Research Report 166, doi: 10.5337/2016.202, 2016.

664 Lacombe, G., Ribolzi, O., de Rouw, A., Pierret, A., Latsachak, K., Silvera, N., Pham Dinh, R.,
665 Orange, D., Janeau, J.-L., Soulileuth, B., Robain, H., Taccoen, A., Sengphaathith, P.,
666 Mouche, E., Sengtaheuanghong, O., Tran Duc, T., and Valentin, C.: Afforestation by
667 natural regeneration or by tree planting: Examples of opposite hydrological impacts
668 evidenced by long-term field monitoring in the humid tropics, *Hydrology and Earth System
669 Sciences Discussions*, 12, 12615-12648, 2015.

670 Leimona, B., Lusiana, B., van Noordwijk, M., Mulyoutami, E., Ekadinata, A., and Amaruzama,
671 S.: Boundary work: knowledge co-production for negotiating payment for watershed
672 services in Indonesia, *Ecosystems Services*, 15, 45–62, 2015.

673 Liu, W., Wei, X., Fan, H., Guo, X., Liu, Y., Zhang, M., and Li, Q.: Response of flow regimes
674 to deforestation and reforestation in a rain-dominated large watershed of subtropical
675 China, *Hydrological Processes*, 29, 5003-5015 , 2015.

676 Lusiana, B., van Noordwijk, M., Suyamto, D., Joshi, L., and Cadisch, G.: Users' perspectives
677 on validity of a simulation model for natural resource management, *International Journal of
678 Agricultural Sustainability*, 9(2), 364-378, 2011.

679 Ma, X., Xu, J. and van Noordwijk, M.: Sensitivity of streamflow from a Himalayan catchment
680 to plausible changes in land cover and climate, *Hydrological Processes*, 24, 1379–1390,
681 2010.

682 Ma, X., Lu, X., van Noordwijk, M., Li, J.T., and Xu, J.C.: Attribution of climate change,
683 vegetation restoration, and engineering measures to the reduction of suspended sediment in
684 the Kejie catchment, southwest China, *Hydrol. Earth Syst. Sci.*, 18, 1979–1994, 2014.

685 Maidment, D.R.: *Handbook of hydrology*, McGraw-Hill Inc., 1992.

686 Malmer, A., Murdiyarso, D., Bruijnzeel L.A., and Ilstedt, U.: Carbon sequestration in tropical
687 forests and water: a critical look at the basis for commonly used generalizations, *Global
688 Change Biology*, 16(2), 599-604, 2010.

689 McCluney, K.E., Poff, N.L., Palmer, M.A., Thorp, J.H., Poole, G.C., Williams, B.S., Williams,
690 M.R., and Baron, J.S.: Riverine macrosystems ecology: sensitivity, resistance, and
691 resilience of whole river basins with human alterations, *Frontiers in Ecology and the
692 Environment*, 12(1), 48-58, 2014.

693 Milly, P.C.D., Wetherald, R., Dunne, K.A., and Delworth, T.L.: Increasing risk of great floods
694 in a changing climate, *Nature*, 415(6871), 514-517, 2002.

695 Palmer, M.A.: Reforming watershed restoration: science in need of application and applications
696 in need of science, *Estuaries and coasts*, 32(1), 1-17, 2009.

697 Rahayu, S., Widodo, R.H., van Noordwijk, M., Suryadi, I., and Verbist, B.: Water monitoring
698 in watersheds. Bogor, Indonesia, World Agroforestry Centre (ICRAF) SEA Regional
699 Program,, 2013

700 Ranieri, S.B.L., Stirzaker, R., Suprayogo, D., Purwanto, E., de Willigen, P., and van Noordwijk,
701 M.: Managing movements of water, solutes and soil: from plot to landscape scale. In: van
702 Noordwijk, M., Cadisch, G. and Ong, C.K. (Eds.) *Belowground Interactions in Tropical
703 Agroecosystems*, CAB International, Wallingford (UK), 329-347, 2004.

704 Richter, B.D., Mathews, R., Harrison, D.L., and Wigington, R.: Ecologically sustainable water
705 management: managing river flows for ecological integrity, *Ecological applications*, 13(1),
706 206-224, 2003.

707 Rodríguez-Iturbe, I. and Rinaldo, A.: *Fractal river basins: chance and self-organization*,
708 Cambridge University Press, Cambridge, 2001.

709 Rose, C.W.: *An introduction to the environmental physics of soil, water and watersheds*.
710 Cambridge University Press, Cambridge (UK) 2004.

711 Rudel, T. K., Coomes, O. T., Moran, E., Achard, F., Angelsen, A., Xu, J., and Lambin, E.:
712 Forest transitions: towards a global understanding of land use change, *Global*
713 *Environmental Change*, 15(1), 23-31, 2005.

714 Seibert, J.: Regionalisation of parameters for a conceptual rainfall-runoff model. *Agricultural*
715 *and Forest Meteorology* 98-99: 279-293, 1999.

716 Seibert, J., Beven, K.J.: Gauging the ungauged basin: how many discharge measurements are
717 needed? *Hydrol. Earth Syst. Sci.*, 13, 883-892, 2009

718 Sloto, R.A. and Crouse, M.Y.: *HYSEP, a computer program for streamflow hydrograph*
719 *separation and analysis*. US Department of the Interior, US Geological Survey, 1996.

720 Sumarga, E., Hein, L., Hooijer, A., and Vernimmen, R.: Hydrological and economic effects of
721 oil palm cultivation in Indonesian peatlands, *Ecology and Society*, 21(2), 2016.

722 Tallaksen, L.M.: A review of baseflow recession analysis, *J Hydrol.*, 165, 349-370, 1995.

723 Tan-Soo, J.S., Adnan, N., Ahmad, I., Pattanayak, S.K., and Vincent, J.R.: Econometric
724 Evidence on Forest Ecosystem Services: Deforestation and Flooding in
725 Malaysia. *Environmental and Resource Economics*, on-line:
726 <http://link.springer.com/article/10.1007/s10640-014-9834-4>, 2014.

727 van de Giesen, N.C., Stomph, T.J., and De Ridder, N.: Scale effects of Hortonian overland flow
728 and rainfall-runoff dynamics in a West African catena landscape, *Hydrological Processes*,
729 14, 165-175, 2000.

730 van Dijk, A.I., van Noordwijk, M., Calder, I.R., Bruijnzeel, L.A., Schellekens, J., and Chappell,
731 N.A.: Forest-flood relation still tenuous – comment on ‘Global evidence that deforestation
732 amplifies flood risk and severity in the developing world’, *Global Change Biology*, 15, 110-
733 115, 2009.

734 van Noordwijk, M., van Roode, M., McCallie, E.L., and Lusiana, B.: Erosion and sedimentation
735 as multiscale, fractal processes: implications for models, experiments and the real world,
736 In: F. Penning de Vries, F. Agus and J. Kerr (Eds.) *Soil Erosion at Multiple Scales*,
737 *Principles and Methods for Assessing Causes and Impacts*. CAB International, Wallingford,
738 223-253, 1998.

739 van Noordwijk, M., Agus, F., Verbist, B., Hairiah, K., and Tomich, T.P.: Managing Watershed
740 Services, In: Scherr, S.J. and McNeely, J.A. (Eds) Ecoagriculture Landscapes. Farming with
741 Nature: The Science and Practice of Ecoagriculture, Island Press, Washington DC, 191 –
742 212, 2007.

743 van Noordwijk, M., Widodo, R.H., Farida, A., Suyamto, D., Lusiana, B., Tanika, L., and
744 Khasanah, N.: GenRiver and FlowPer: Generic River and Flow Persistence Models. User
745 Manual Version 2.0. Bogor, Indonesia, World Agroforestry Centre (ICRAF) Southeast Asia
746 Regional Program, 2011.

747 van Noordwijk, M., Leimona, B., Jindal, R., Villamor, G.B., Vardhan, M., Namirembe, S.,
748 Catacutan, D., Kerr, J., Minang, P.A., and Tomich, T.P.: Payments for Environmental
749 Services: evolution towards efficient and fair incentives for multifunctional landscapes,
750 Annu. Rev. Environ. Resour., 37, 389-420, 2012.

751 van Noordwijk, M., Lusiana, B., Leimona, B., Dewi, S., and Wulandari, D.: Negotiation-
752 support toolkit for learning landscapes, Bogor, Indonesia, World Agroforestry Centre
753 (ICRAF) Southeast Asia Regional Program, 2013.

754 van Noordwijk, M., Leimona, B., Xing, M., Tanika, L., Namirembe, S., and Suprayogo, D.:
755 Water-focused landscape management. Climate-Smart Landscapes: Multifunctionality In
756 Practice. eds Minang PA et al.. Nairobi, Kenya, World Agroforestry Centre (ICRAF), 179-
757 192, 2015a.

758 van Noordwijk, M., Bruijnzeel, S., Ellison, D., Sheil, D., Morris, C., Gutierrez, V., Cohen, J.,
759 Sullivan, C., Verbist, B., and Muys, B.: Ecological rainfall infrastructure: investment in
760 trees for sustainable development, ASB Brief no 47. Nairobi. ASB Partnership for the
761 Tropical Forest Margins, 2015b.

762 van Noordwijk M, Kim Y-S, Leimona B, Hairiah K, Fisher LA,: Metrics of water security,
763 adaptive capacity and agroforestry in Indonesia. Current Opinion on Environmental
764 Sustainability (in press: <http://dx.doi.org/10.1016/j.cosust.2016.10.004>), 2016.

765 Verbist, B., Poesen, J., van Noordwijk, M. Widianto, Suprayogo, D., Agus, F., and Deckers, J.:
766 Factors affecting soil loss at plot scale and sediment yield at catchment scale in a tropical
767 volcanic agroforestry landscape, Catena, 80, 34-46, 2010.

768 Ward, R.C. and Robinson, M.: *Principles of hydrology*. 4th edition. New York: McGraw-Hill,
769 2000.

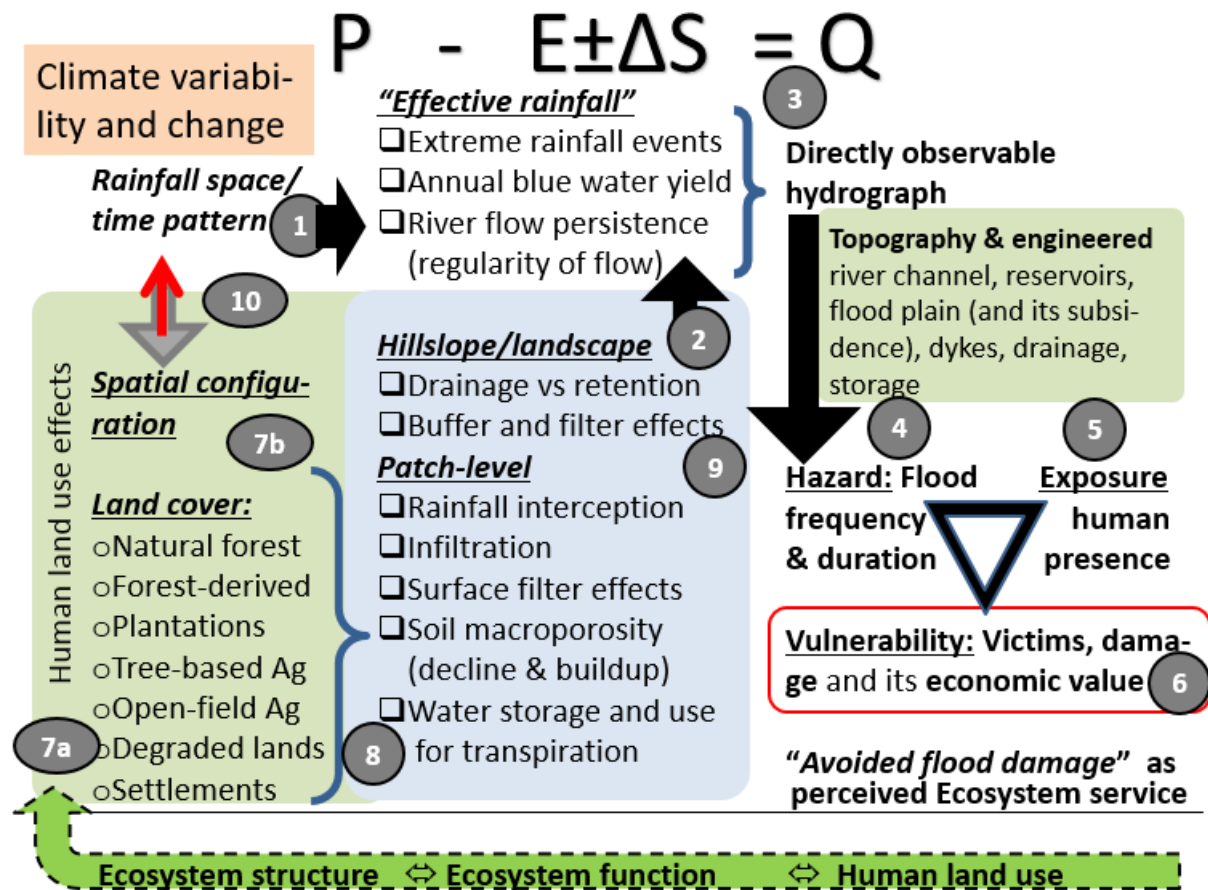
770 Weiler, M. and McDonnell, J.: Virtual experiments: a new approach for improving process
771 conceptualization in hillslope hydrology, *Journal of Hydrology*, 285(1), 3-18, 2004

772 Winsemius, H.C., van Beek, L.P.H., Jongman, B., Ward, P.J., and Bouwman, A.: A
773 framework for global river flood risk assessments, *Hydrol Earth Syst Sci*, 17,1871–1892,
774 2013.

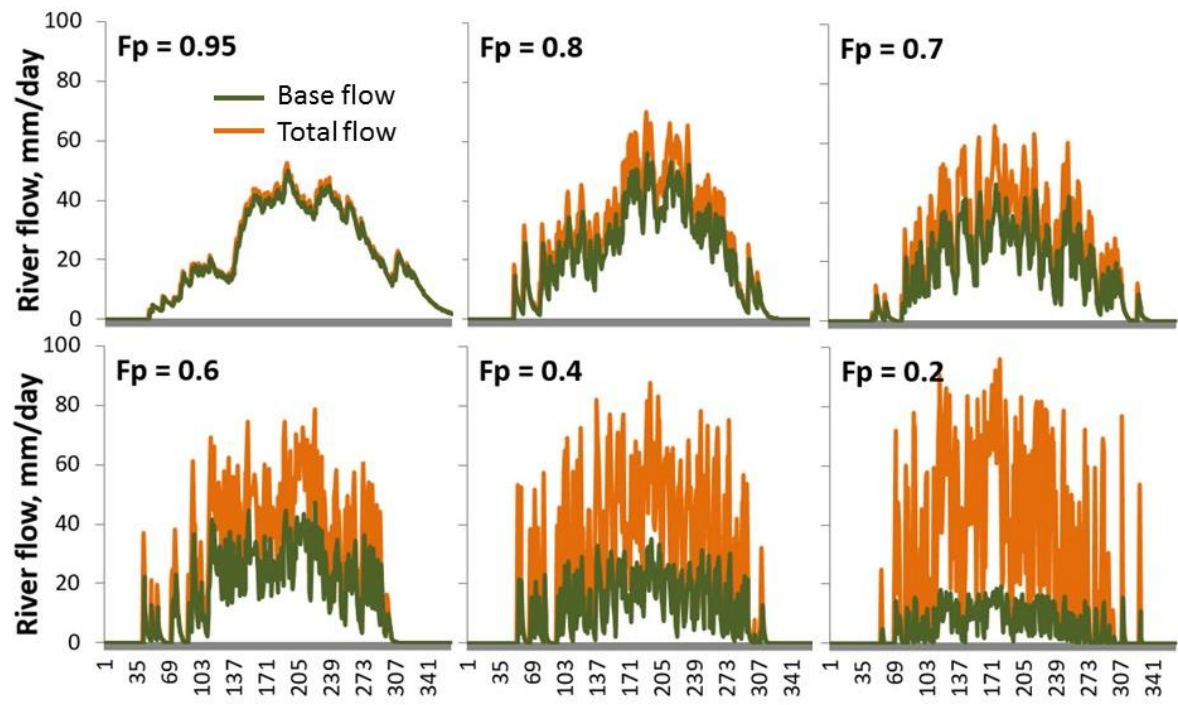
775 Yen, H., White, M.J., Jeong, J., Arabi, M. and Arnold, J.G.: Evaluation of alternative surface
776 runoff accounting procedures using the SWAT model, *International Journal of Agricultural
777 and Biological Engineering*, 8(3), 54-68, 2015.

778 Zhou, G., Wei, X., Luo, Y., Zhang, M., Li, Y., Qiao, Y., Liu, H., and Wang, C.: Forest recovery
779 and river discharge at the regional scale of Guangdong Province, China, *Water Resources
780 Research*, 46(9), W09503, doi:10.1029/2009WR00829, 2010.

781

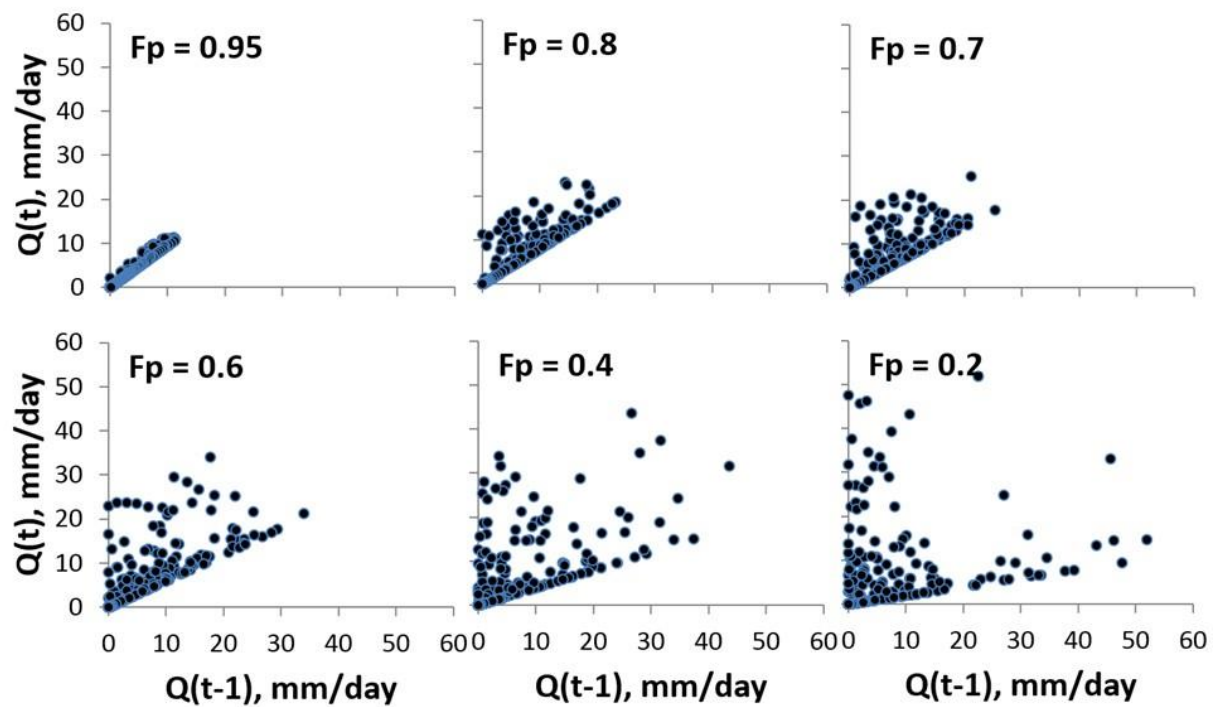


784 Figure 1. Steps in a causal pathway that relates rainfall (1) via watershed conditions (2) to the
 785 pattern of river flow described in a hydrograph (3), which can get modified by the conditions
 786 along the river channel into a hazard of flood frequency and duration (4); jointly with
 787 exposure (being in the wrong place at critical times, 5) and vulnerability (6) this determines
 788 flood damage; in avoiding flood damage, the condition in the watershed with its landcover
 789 and spatial configuration (7) influences the patch level water partitioning over overland flow
 790 and infiltration (8), while hillslope level configuration further influences flow pathways (9)
 791 and land cover potentially influences rainfall (10)



796 Figure 2. Example of daily river flow, split into a base flow and additional flow component, for
 797 a unimodal sinus-based rainfall probability multiplied with a rainfall depth calculated as
 798 $60^{\text{rand}(0.1)}$ mm/day (~120 rainy days, annual $Q \sim 1600$ mm) in watersheds characterized
 799 by F_p values ranging from 0.95 to 0.2

801



802

803 Figure 3. Biplots of $Q(t)$ versus $Q(t-1)$ for the same simulations as Figure 2

804

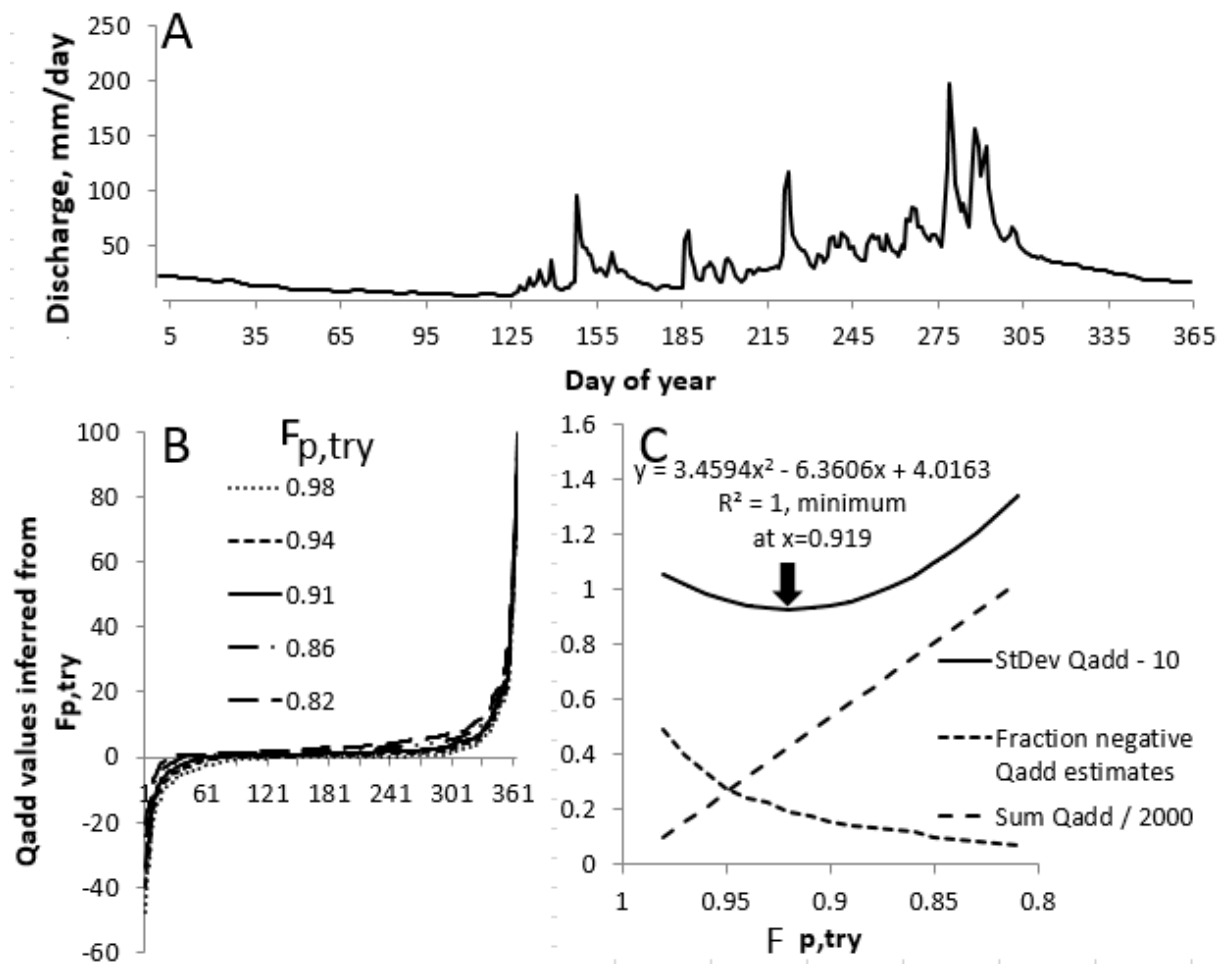
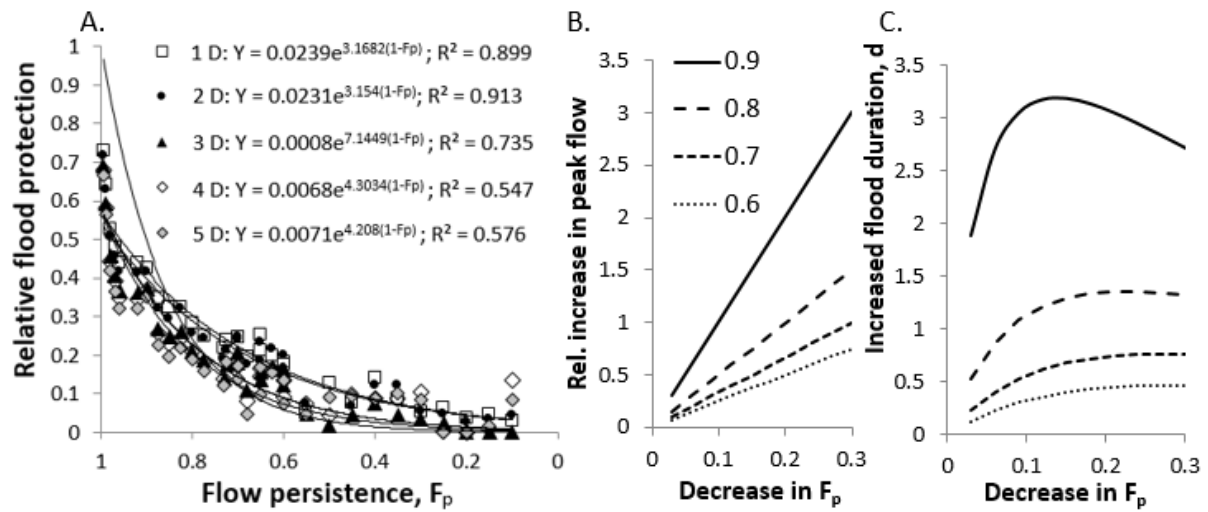
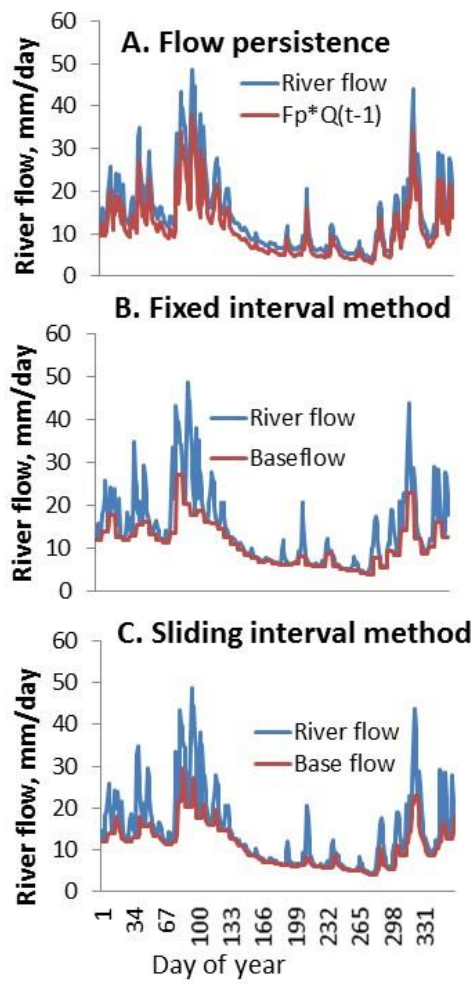


Figure 4. Example of the derivation of best fitting $F_{p,try}$ value for an example hydrograph (A) on the basis of the inferred Q_a distribution (cumulative frequency in B), and three properties of this distribution (C): its sum, frequency of negative values and standard deviation; the $F_{p,try}$ minimum of the latter is derived from the parameters of a fitted quadratic equation

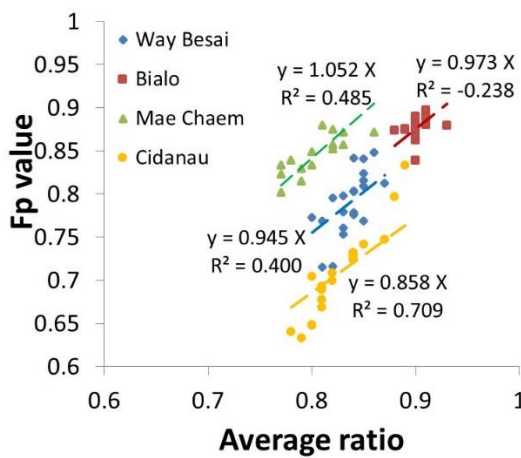


812
813
814 Figure 5. A. Effects of flow persistence on the relative flood protection (decrease in maximum
815 flow measured over a 1 – 5 d period relative to a case with $F_p = 0$ (a few small negative
816 points were replaced by small positive values to allow the exponential fit); B and C. effects
817 of a decrease in flow persistence on the volume of water involved in peak flows (B;
818 relative to the volume at F_p is 0.6 – 0.9) and in the duration (in d) of floods (C)
819



820
821
822
823

Figure 6. Comparison of baseflow separation of a hydrograph according to the flow persistence method (A) and two common flow separation methods, respectively with fixed (B) and sliding intervals (C)



824
825
826
827
828

Figure 7. Comparison of yearly data for four watersheds (see paper II) analysed with common flow separation methods (as in Fig. 6) and the flow persistence method

829 Flood risk reduction and flow buffering as ecosystem services:
830 II. Land use and rainfall intensity effects in Southeast Asia

831 Meine van Noordwijk^{1,2}, Lisa Tanika¹, Betha Lusiana¹ [1]{World Agroforestry Centre
832 (ICRAF), SE Asia program, Bogor, Indonesia}

833 [2]{Wageningen University, Plant Production Systems, Wageningen, the Netherlands}

834 Correspondence to: Meine van Noordwijk (m.vannoordwijk@cgiar.org)

835 **Abstract**

836 The way watersheds buffer the temporal pattern of river flow relative to the temporal
837 pattern of rainfall is an important ecosystem service. Part of this buffering is inherent to
838 its geology and climate, but another part is responding to human use and misuse of the
839 landscape, and can be part of management feedback loops if salient, credible and
840 legitimate indicators can be found and used. Dissecting the anthropogenic change from
841 exogenous variability (e.g. the specific time-space pattern of rainfall during an
842 observation period) is relevant for designing and monitoring of watershed management
843 interventions. Part I introduced the concept of flow persistence, key to a parsimonious
844 recursive model of river flow. It also discussed the operational derivation of the F_p
845 parameter. Here we compare F_p estimates from four meso-scale watersheds in Indonesia
846 (Cidanau, Way Besai, and Bialo) and Thailand (Mae Chaem), with varying climate,
847 geology and land cover history, at a decadal time scale. The likely response in each of
848 these four to variation in rainfall properties (incl. the maximum hourly rainfall intensity)
849 and land cover (comparing scenarios with either more or less forest and tree cover than
850 the current situation) was explored through a basic daily water balance model,
851 GenRiver. This model was calibrated for each site on existing data, before being used
852 to explore alternative land cover and rainfall parameter settings. In both data and model
853 runs, the wet-season (3-monthly) F_p values were consistently lower than dry-season
854 values for all four sites. Across the four catchments F_p values decreased with increasing
855 annual rainfall, but specific aspects of watersheds, such as the riparian swamp (peat
856 soils) in Cidanau reduced effects of land use change in the upper watershed. Increasing
857 the mean rainfall intensity (at constant monthly totals for rainfall) around the values
858 considered typical for each landscape was predicted to decrease F_p values by between

859 0.047 (Bialo) and 0.261 (Mae Chaem). Sensitivity of F_p to changes in land use change
860 plus changes in rainfall intensity depends on other characteristics of the watersheds, and
861 generalizations made on the basis of one or two case studies may not hold, even within
862 the same climatic zone. A wet-season F_p value above 0.7 was achievable in forest-
863 agroforestry mosaic case studies. Interannual variability in F_p was found to be large
864 relative to effects of land cover change and likely reflects sensitivity in the model of
865 Hortonian overland flow to variations in rainfall intensity. Multiple (5-10) years of
866 paired-plot data would generally be needed to reject no-change null-hypotheses on the
867 effects of land use change (degradation and restoration). While empirical evidence of
868 such effects at scale is understandably scarce, F_p trends over time serve as a holistic
869 scale-dependent performance indicator of degrading/recovering watershed health and
870 can be tested for acceptability and acceptance in a wider socio-ecological context.

871 **Introduction**

872 Inherent properties (geology, geomorphology) interact with climate and human modification of
873 vegetation, soils, drainage and riparian wetlands in the degree of buffering that watersheds
874 provide (Andréassian 2004; Bruijnzeel, 2004). Buffering of river flow relative to the space-time
875 dynamics of rainfall is an ecosystem service, reducing the exposure of people living on
876 geomorphological floodplains to high-flow events, and increasing predictability and river flow
877 in dry periods (Joshi et al., 2004; Leimona et al., 2015; Part I). In the absence of any vegetation
878 and with a sealed surface, river flow will directly respond to the spatial distribution of rainfall,
879 with only the travel time to any point of specific interest influencing the temporal pattern of
880 river flow. Any persistence or predictability of river flow in such a situation will reflect
881 temporal autocorrelation of rainfall, beyond statistical predictability in seasonal rainfall
882 patterns. On the other side of the spectrum, river flow can be constant every day, beyond the
883 theoretical condition of constant rainfall, in a watershed that provides perfect buffering, by
884 passing all water through groundwater pools that have sufficient storage capacity at any time
885 during the year. Both infiltration-limited (Hortonian) and saturation-induced use of more rapid
886 flow pathways (inter and overland flows) will reduce the flow persistence and make it, at least
887 in part, dependent on rainfall events. Separating the effects of land cover (land use), engineering
888 and rainfall on the actual flow patterns of rivers remains a considerable challenge (Ma et al.,
889 2014; Verbist et al., 2019). It requires data, models and concepts that can serve as effective
890 boundary object in communication with stakeholders (Leimona et al. 2015; van Noordwijk et

891 al. 2012). There is a long tradition in using forest cover as such a boundary object, but there is
892 only a small amount of evidence supporting this (Tan-Soo et al., 2014; van Dijk et al., 2009;
893 van Noordwijk et al. 2015a).

894 In part I, we introduced a flow persistence parameter (F_p) that links the two, asymmetrical
895 aspects of flow dynamics: translating rainfall excess into river flow, and gradually releasing
896 water stored in the landscape. Here, in part II we will apply the F_p algorithm to river flow data
897 for a number of contrasting meso-scale watersheds in Southeast Asia. These were selected to
898 represent variation in rainfall and land cover, and test the internal consistency of results based
899 on historical data: two located in the humid and one in the subhumid tropics of Indonesia, and
900 one in the unimodal subhumid tropics of northern Thailand.

901 After exploring the patterns of variation in F_p estimates derived from river flow records, we
902 will quantify the sensitivity of the F_p metric to variations in rainfall intensity and its response,
903 on a longer timescale to land cover change. To do so, we will use a model that uses basic water
904 balance concepts: rainfall interception, infiltration, water use by vegetation, overland flow,
905 interflow and groundwater release, to a spatially structured watershed where travel time from
906 sub watersheds to any point of interest modifies the predicted river flow. In the specific model
907 used land cover effects on soil conditions, interception and seasonal water use have been
908 included. After testing whether F_p values derived from model outputs match those based on
909 empirical data where these exist, we rely on the basic logic of the model to make inference on
910 the relative importance of modifying rainfall and land cover inputs. With the resulting temporal
911 variation in calculated F_p values, we consider the time frame at which observed shifts in F_p can
912 be attributed to factors other than chance (that means: null-hypotheses of random effects can be
913 rejected with accepted chance of Type I errors).

914 **2. Methods**

915 **2.1 GenRiver model for effects of land cover on river flow**

916 The GenRiver model (van Noordwijk et al., 2011) is based on a simple water balance concept
917 with a daily time step and a flexible spatial subdivision of a watershed that influences the
918 routing of water and employs spatially explicit rainfall. At patch level, vegetation influences
919 interception, retention for subsequent evaporation and delayed transfer to the soil surface, as
920 well as the seasonal demand for water. Vegetation (land cover) also influences soil porosity and
921 infiltration, modifying the inherent soil properties. Water in the root zone is modelled separately
922 for each land cover within a subcatchment, the groundwater stock is modelled at subcatchment

923 level. The spatial structure of a watershed and the routing of surface flows influences the time
924 delays to any specified point of interest, which normally includes the outflow of the catchment.
925 Land cover change scenarios are interpolated annually between time-series (measured or
926 modelled) data. The model may use measured rainfall data, or use a rainfall generator that
927 involves Markov chain temporal autocorrelation (rain persistence). As our data sources are
928 mostly restricted to daily rainfall measurements and the infiltration model compares
929 instantaneous rainfall to infiltration capacity, a stochastic rainfall intensity was applied at
930 subcatchment level, driven by the mean as parameter and a standard deviation for a normal
931 distribution (truncated at 3 standard deviations from the mean) proportional to it via a
932 coefficient of variation as parameter. For the Mae Chaem site in N Thailand data by Dairaku et
933 al. (2004) suggested a mean of less than 3 mm/hr. For the three sites in Indonesia we used 30
934 mm/hr, based on Kusumastuti et al. (2016). Appendix 1 provides further detail on the GenRiver
935 model. The model itself, a manual and application case studies are freely available
936 (<http://www.worldagroforestry.org/output/genriver-genetic-river-model-river-flow>; van
937 Noordwijk et al., 2011).

938 **2.2 Empirical data-sets, model calibration**

939 Table 1 and Figure 1 provide summary characteristics and the location of river flow data used
940 in four meso-scale watersheds for testing the F_p algorithm and application of the GenRiver
941 model. Figure 1 includes a water tower category in the agro-ecological zones; this is defined on
942 the basis of a ratio of precipitation and potential evapotranspiration of more than 0.65, and a
943 product of that ratio and relative elevation exceeding 0.277.

944 ⇒ Table 1
945 ⇒ Figure 1

946 As major parameters for the GenRiver model were not independently measured for the
947 respective watersheds, we tuned (calibrated) the model by modifying parameters within a
948 predetermined plausible range, and used correspondence with measured hydrograph as test
949 criterion (Kobolt et al. 2008). We used the Nash-Sutcliff Efficiency (NSE) parameter (target
950 above 0.5) and bias (less than 25%) as test criteria and targets. Meeting these performance
951 targets (Moriasi et al., 2007), we accepted the adjusted models as basis for describing current
952 conditions and exploring model sensitivity. The main site-specific parameter values are listed
953 in Table 2 and (generic) land cover specific default parameters in Table 3.

954 ⇒ Table 2
955 ⇒ Table 3

956 Table 4 describes the six scenarios of land use change that were evaluated in terms of their
957 hydrological impacts. Further description on the associated land cover distribution for each
958 scenario in the four different watersheds is depicted in Appendix 2.

959 \Rightarrow Table 4

960 **2.3 Bootstrapping to estimate the minimum observation**

961 The bootstrap methods (Efron and Tibshirani, 1986) is a resampling methods that is commonly
962 used to generate ‘surrogate population’ for the purpose of approximating the sampling
963 distribution of a statistic. In this study, the bootstrap approach was used to estimate the
964 minimum number of observation (or yearly data) required for a pair-wise comparison test
965 between two time-series of stream flow or discharge data (representing two scenarios of land
966 use distributions) to be distinguishable from a null-hypothesis of no effect. The pair-wise
967 comparison test used was Kolmogorov-Smirnov test that is commonly used to test the
968 distribution of discharge data (Zhang et al, 2006). We built a simple macro in R (R Core Team,
969 2015) that entails the following steps:

- 970 (i) Bootstrap or resample with replacement 1000 times from both time-series discharge
971 data with sample size n ;
- 972 (ii) Apply the Kolmogorov-Smirnov test to each of the 1000 generated pair-wise discharge
973 data, and record the P-value;
- 974 (iii) Perform (i) and (ii) for different size of n , ranging from 5 to 50.
- 975 (iv) Tabulate the p-value from the different sample size n , and determine the value of n when
976 the p-value reached equal to or less than 0.025 (or equal to the significance level of 5%).
977 The associated n represents the minimum number of observations required.

978 Appendix 3 provides an example of the macro in R used for this analysis.

979 **3. Results**

980 **3.1 Empirical data of flow persistence as basis for model parameterization**

981 Inter-annual variability of F_p estimates derived for the four catchments (Figure 2) was of the
982 order of 0.1 units, while the intra-annual variability between dry and rainy seasons was 0.1-0.2.
983 For all for the years and locations, rainy season F_p values, with mixed flow pathways, were
984 consistently below dry-season values, dominated by groundwater flows. If we can expect $F_{p,i}$
985 and $F_{p,o}$ (see equation 8 in part I) to be approximately 0.5 and 0, this difference between wet

986 and dry periods implies a 40% contribution of interflow in the wet season, a 20% contribution
987 of overland flow or any combination of the two effects.

988 Overall the estimates from modelled and observed data are related with 16% deviating more
989 than 0.1 and 3% more than 0.15 (Figure 3). As the Moriasi et al. (2007) performance criteria
990 for the hydrographs were met by the calibrated models for each site, we tentatively accept the
991 model to be a basis for sensitivity study of F_p to modifications to land cover and/or rainfall

992 \Rightarrow Figure 2

993 \Rightarrow Figure 3

994 **3.2 Comparing F_p effects of rainfall intensity and land cover change**

995 A direct comparison of model sensitivity to changes in mean rainfall intensity and land use
996 change scenarios is provided in Figure 4. Varying the mean rainfall intensity over a factor 7
997 shifted the F_p value by only 0.047 and 0.059 in the case of Bialo and Cidanau, respectively, but
998 by 0.128 in Way Besai and 0.261 in Mae Chaem (Figure 4A). The impact of the land use change
999 scenarios on F_p was smallest in Cidanau (0.026), intermediate in Way Besai (0.048) and
1000 relatively large in Bialo and Mae Chaem, at 0.080 and 0.084, respectively (Figure 4B). The
1001 order of F_p across the land use change scenarios was mostly consistent between the watersheds,
1002 but the contrast between the ReFor and NatFor scenario was largest in Mae Chaem and smallest
1003 in Way Besai. In Cidanau, Way Besai and Mae Chaem, variations in rainfall were 2.2 to 3.1
1004 times more effective than land use change in shifting F_p , in Bialo its relative effect was only
1005 58%. Apparently, the sensitivity to changes in land use change plus changes in rainfall intensity
1006 depends on other characteristics of the watersheds, and generalizations made on the basis of
1007 one or two case studies may not hold, even within the same climatic zone.

1008 \Rightarrow Figure 4

1009 **3.3 Further analysis of F_p effects for scenarios of land cover change**

1010 Among the four watersheds there is consistency in that the 'forest' scenario has the highest, and
1011 the 'degraded lands' the lowest F_p value (Figure 5), but there are remarkable differences as well:
1012 in Cidanau the interannual variation in F_p is clearly larger than land cover effects, while in the
1013 Way Besai the spread in land use scenarios is larger than interannual variability. In Cidanau a
1014 peat swamp between most of the catchment and the measuring point buffers most of landcover
1015 related variation in flow, but not the interannual variability. Considering the frequency
1016 distributions of F_p values over a 20 year period, we see one watershed (Way Besai) where the
1017 forest stands out from all others, and one (Bialo) where the degraded lands are separate from

1018 the others. Given the degree of overlap of the frequency distributions, it is clear that multiple
1019 years of empirical observations will be needed before a change can be affirmed.

1020 Figure 5 shows the frequency distributions of expected effect sizes on F_p of a comparison of
1021 any land cover with either forest or degraded lands. Table 5 translates this information to the
1022 number of years that a paired plot (in the absence of measurement error) would have to be
1023 maintained to reject a null-hypothesis of no effect, at $p=0.05$. As the frequency distributions of
1024 F_p differences of paired catchments do not match a normal distribution, a Kolmogorov-Smirnov
1025 test can be used to assess the probability that a no-difference null hypothesis can yield the
1026 difference found. By bootstrapping within the years where simulations supported by observed
1027 rainfall data exist, we found for the Way Besai catchment, for example, that 20 years of data
1028 would be needed to assert (at $P = 0.05$) that the ReFor scenario differs from AgFor, and 16
1029 years that it differs from Actual and 11 years that it differs from Degrade. In practice, that means
1030 that empirical evidence that survives statistical tests will not emerge, even though effects on
1031 watershed health are real.

1032 ⇒ Figure 5
1033 ⇒ Table 5

1034 At process-level the increase in 'overland flow' in response to soil compaction due to land cover
1035 change has a clear and statistically significant relationship with decreasing F_p values in all
1036 catchments (Figure 6), but both year-to-year variation within a catchment and differences
1037 between catchments influence the results as well, leading to considerable spread in the biplot.
1038 Contrary to expectations, the disappearance of 'interflow' by soil compaction is not reflected in
1039 measurable change in F_p value. The temporal difference between overland and interflow (one
1040 or a few days) gets easily blurred in the river response that integrates over multiple streams with
1041 variation in delivery times; the difference between overland- or interflow and baseflow is much
1042 more pronounced. Apparently, according to our model, the high macroporosity of forest soils
1043 that allows interflow and may be the 'sponge' effect attributed to forest, delays delivery to rivers
1044 by one or a few days, with little effect on the flow volumes at locations downstream where flow
1045 of multiple days accumulates. The difference between overland- or interflow and baseflow in
1046 time-to-river of rainfall peaks is much more pronounced.

1047 ⇒ Figure 6

1048 Tree cover has two contradicting effects on baseflow: it reduces the surplus of rainfall over
1049 evapotranspiration (annual water yield) by increased evapotranspiration (especially where
1050 evergreen trees are involved), but it potentially increases soil macroporosity that supports

1051 infiltration and interflow, with relatively little effect on water holding capacity measured as
1052 'field capacity' (after runoff and interflow have removed excess water). Figure 7 shows that the
1053 total volume of baseflow differs more between sites and their rainfall pattern than it varies with
1054 tree cover. Between years total evapotranspiration and baseflow totals are positively correlated,
1055 but for a given rainfall there is a trade-off. Overall these results support the conclusion that
1056 generic effects of deforestation on decreased flow persistence, and of (agro)/(re)-forestation on
1057 increased flow persistence are small relative to interannual variability due to specific rainfall
1058 patterns, and that it will be hard for any empirical data process to pick-up such effects, even if
1059 they are qualitatively aligned with valid process-based models.

1060 \Rightarrow Figure 7

1061 **4. Discussion**

1062 In the discussion of Part I the credibility questions on replicability of the F_p metric and its
1063 sensitivity to details of rainfall pattern versus land cover as potential causes of variation were
1064 seen as requiring case studies in a range of contexts. Although the four case studies in Southeast
1065 Asia presented here cannot be claimed to represent the global variation in catchment behaviour
1066 (with absence of a snowpack and its dynamics as an obvious element of flow buffering not
1067 included), the diversity of responses among these four already point to challenges for any
1068 generic interpretation of the degree of flow persistence that can be achieved under natural forest
1069 cover, as well as its response to land cover change.

1070 The empirical data summarized here for (sub)humid tropical sites in Indonesia and Thailand
1071 show that values of F_p above 0.9 are scarce in the case studies provided, but values above 0.8
1072 were found, or inferred by the model, for forested landscapes. Agroforestry landscapes
1073 generally presented F_p values above 0.7, while open-field agriculture or degraded soils led to F_p
1074 values of 0.5 or lower. Due to differences in local context, it may not be feasible to relate typical
1075 F_p values to the overall condition of a watershed, but temporal change in F_p can indicate
1076 degradation or restoration if a location-specific reference can be found. The difference between
1077 wet and dry season F_p can be further explored in this context. The dry season F_p value primarily
1078 reflects the underlying geology, with potential modification by engineering and operating rules
1079 of reservoirs, the wet season F_p is generally lower due to partial shifts to overland and interflow
1080 pathways. Where further uncertainty is introduced by the use of modelled rather than measured
1081 river flow, the lack of fit of models similar to the ones we used here would mean that scenario
1082 results are indicative of directions of change rather than a precision tool for fine-tuning

1083 combinations of engineering and land cover change as part of integrated watershed
1084 management.

1085 The differences in relative response of the watersheds to changes in mean rainfall intensity and
1086 land cover change, suggest that generalizations derived from one or a few case studies are to be
1087 interpreted cautiously. If land cover change would influence details of the rainfall generation
1088 process (arrow 10 in Figure 1 of part I; e.g. through release of ice-nucleating bacteria Morris et
1089 al., 2014; van Noordwijk et al., 2015b) this can easily dominate over effects via interception,
1090 transpiration and soil changes.

1091 Our results indicate an intra-annual variability of F_p values between wet and dry seasons of
1092 around 0.2 in the case studies, while interannual variability in either annual or seasonal F_p was
1093 generally in the 0.1 range. The difference between observed and simulated flow data as basis
1094 for F_p calculations was mostly less than 0.1. With current methods, it seems that effects of land
1095 cover change on flow persistence that shift the F_p value by about 0.1 are the limit of what can
1096 be asserted from empirical data (with shifts of that order in a single year a warning sign rather
1097 than a firmly established change). When derived from observed river flow data F_p is suitable
1098 for monitoring change (degradation, restoration) and can be a serious candidate for monitoring
1099 performance in outcome-based ecosystem service management contracts.

1100 In view of our results the lack of robust evidence in the literature of effects of change in forest
1101 and tree cover on flood occurrence may not be a surprise; effects are subtle and most data sets
1102 contain considerable variability. Yet, such effects are consistent with current process and
1103 scaling knowledge of watersheds.

1104 **Conclusion**

1105 Overall, our analysis suggests that the level of flow buffering achieved depends on both land
1106 cover (including its spatial configuration and effects on soil properties) and space-time patterns
1107 of rainfall (including maximum rainfall intensity as determinant of overland flow).
1108 Generalizations on dominant influence of either, derived from one or a few case studies are to
1109 be interpreted cautiously. If land cover change would influence details of the rainfall generation
1110 process this can easily dominate over effects via interception, transpiration and soil changes.
1111 Multi-year data will generally be needed to attribute observed changes in flow buffering to
1112 degradation/restoration of watersheds, rather than specific rainfall events. With current
1113 methods, it seems that effects of land cover change on flow persistence that shift the F_p value

1114 by about 0.1 are the limit of what can be asserted from empirical data, with shifts of that order
1115 in a single year a warning sign rather than a firmly established change. When derived from
1116 observed river flow data F_p is suitable for monitoring change (degradation, restoration) and can
1117 be a serious candidate for monitoring performance in outcome-based ecosystem service
1118 management contracts.

1119 Further tests on the performance of the F_p metric and its standard incorporation into the output
1120 modules of river flow and watershed management models will broaden the basis for interpreting
1121 the value ranges that can be expected for well-functioning watersheds in various conditions of
1122 climate, topography, soils, vegetation and engineering interventions. Such a broader empirical
1123 base could test the possible use of F_p as performance metric for watershed rehabilitation efforts.

1124 **Data availability**

1125 Table 6 specifies the rainfall and river flow data we used for the four basins and specifies the
1126 links to detailed descriptions.

1127 \Rightarrow Table 6

1128 **Acknowledgements**

1129 This research is part of the Forests, Trees and Agroforestry research program of the CGIAR.
1130 Several colleagues contributed to the development and early tests of the F_p method. Thanks are
1131 due to Thoha Zulkarnain for assistance with Figure 1 and to Eike Luedeling, Sonya Dewi,
1132 Sampurno Bruijnzeel and two anonymous reviewers for comments on an earlier version of the
1133 manuscript.

1134 **References**

1135 Andréassian, V.: Waters and forests: from historical controversy to scientific debate, *Journal of*
1136 *Hydrology*, 291, 1–27, 2004.

1137 Bruijnzeel, L.A.: Hydrological functions of tropical forests: not seeing the soil for the trees,
1138 *Agr. Ecosyst. Environ.*, 104, 185–228, 2004.

1139 Dairaku K., Emori, S., and Taikan, T.: Rainfall Amount, Intensity, Duration, and Frequency
1140 Relationships in the Mae Chaem Watershed in Southeast Asia, *Journal of*
1141 *Hydrometeorology*, 5, 458-470, 2004.

1142 Efron, B and Tibshirani, R.: Bootstrap Methods for Standard Errors, Confidence Intervals, and
1143 Other Measures of Statistical Accuracy. *Statistical Science* 1 (1): 54-75, 1986.

1144 Joshi, L., Schalenbourg, W., Johansson, L., Khasanah, N., Stefanus, E., Fagerström, M.H., and
1145 van Noordwijk, M.: Soil and water movement: combining local ecological knowledge with
1146 that of modellers when scaling up from plot to landscape level, In: van Noordwijk, M.,
1147 Cadisch, G. and Ong, C.K. (Eds.) *Belowground Interactions in Tropical Agroecosystems*,
1148 CAB International, Wallingford (UK), 349-364, 2004.

1149 Kobold, M., Suselj, K., Polajnar, J., and Pogacnik, N.: Calibration Techniques Used For HBV
1150 Hydrological Model In Savinja Catchment, In: XXIVth Conference of the Danubian
1151 Countries On The Hydrological Forecasting And Hydrological Bases Of Water
1152 Management, 2008.

1153 Kusumastuti, D.I., Jokowinarno, D., van Rafi'i, C.H., and Yuniarti, F.: Analysis of rainfall
1154 characteristics for flood estimation in Way Awi watershed, Civil Engineering Dimension,
1155 18, 31-37, 2016

1156 Leimona, B., Lusiana, B., van Noordwijk, M., Mulyoutami, E., Ekadinata, A., and Amaruzama,
1157 S.: Boundary work: knowledge co-production for negotiating payment for watershed
1158 services in Indonesia, *Ecosystems Services*, 15, 45–62, 2015.

1159 Ma, X., Lu, X., van Noordwijk, M., Li, J.T., and Xu, J.C.: Attribution of climate change,
1160 vegetation restoration, and engineering measures to the reduction of suspended sediment in
1161 the Kejie catchment, southwest China, *Hydrol. Earth Syst. Sci.*, 18, 1979–1994, 2014.

1162 Moriasi, D.N., Arnold, J.G., Van Liew, M.W., Bingner, R.L., Harmel, R.D., and Veith, T.L.:
1163 Model Evaluation Guidelines For Systematic Quantification Of Accuracy In Watershed
1164 Simulations, American Society of Agricultural and Biological Engineers, 20(3),885-900,
1165 2001

1166 Morris, C.E., Conen, F., Huffman, A., Phillips, V., Pöschl, U., and Sands, D.C.:
1167 Bioprecipitation: a feedback cycle linking Earth history, ecosystem dynamics and land use
1168 through biological ice nucleators in the atmosphere, *Glob Change Biol*, 20, 341-351.
1169 2014.

1170 R Core Team R: A language and environment for statistical computing. R Foundation for
1171 Statistical Computing, Vienna, Austria, URL <http://www.R-project.org/>, 2015

1172 Tan-Soo, J.S., Adnan, N., Ahmad, I., Pattanayak, S.K., and Vincent, J.R.: Econometric
1173 Evidence on Forest Ecosystem Services: Deforestation and Flooding in Malaysia.
1174 Environmental and Resource Economics, on-line:
1175 <http://link.springer.com/article/10.1007/s10640-014-9834-4>, 2014.

1176 van Dijk, A.I., van Noordwijk, M., Calder, I.R., Bruijnzeel, L.A., Schellekens, J., and Chappell,
1177 N.A.: Forest-flood relation still tenuous – comment on ‘Global evidence that deforestation
1178 amplifies flood risk and severity in the developing world’, *Global Change Biology*, 15, 110-
1179 115, 2009.

1180 van Noordwijk, M., Widodo, R.H., Farida, A., Suyamto, D., Lusiana, B., Tanika, L., and
1181 Khasanah, N.: GenRiver and FlowPer: Generic River and Flow Persistence Models. User
1182 Manual Version 2.0, Bogor, Indonesia, World Agroforestry Centre (ICRAF) Southeast Asia
1183 Regional Program, 2011.

1184 van Noordwijk, M., Leimona, B., Jindal, R., Villamor, G.B., Vardhan, M., Namirembe, S.,
1185 Catacutan, D., Kerr, J., Minang, P.A., and Tomich, T.P.: Payments for Environmental
1186 Services: evolution towards efficient and fair incentives for multifunctional landscapes,
1187 *Annu. Rev. Environ. Resour.*, 37, 389-420, 2012.

1188 van Noordwijk, M., Leimona, B., Xing, M., Tanika, L., Namirembe, S., and Suprayogo, D.:
1189 Water-focused landscape management. *Climate-Smart Landscapes: Multifunctionality In*
1190 *Practice*, eds Minang PA et al.. Nairobi, Kenya: World Agroforestry Centre (ICRAF), 179-
1191 192, 2015a.

1192 van Noordwijk, M., Bruijnzeel, S., Ellison, D., Sheil, D., Morris, C., Gutierrez, V., Cohen, J.,
1193 Sullivan, C., Verbist, B., and Muys, B.: Ecological rainfall infrastructure: investment in
1194 trees for sustainable development, *ASB Brief no 47*, Nairobi, ASB Partnership for the
1195 Tropical Forest Margins, 2015b.

1196 Verbist, B., Poesen, J., van Noordwijk, M. Widianto, Suprayogo, D., Agus, F., and Deckers, J.:
1197 Factors affecting soil loss at plot scale and sediment yield at catchment scale in a tropical
1198 volcanic agroforestry landscape, *Catena*, 80, 34-46, 2010.

1199 Zhang, Q., Liu, C., Xu, C., Xu, and Jiang T.: Observed trends of annual maximum water level
1200 and streamflow during past 130 years in the Yangtze River basin, China, *Journal of*
1201 *Hydrology*, 324, 255-265, 2006.

1202

1203 Table 1. Basic physiographic characteristics of the four study watersheds

Parameter	Bialo	Cidanau	Mae Chaem	Way Besai
Location	South Sulawesi, Indonesia	West Java, Indonesia	Northern Thailand	Lampung, Sumatera, Indonesia
Coordinates	5.43 S, 120.01 E	6.21 S, 105.97 E	18.57 N, 98.35 E	5.01 S, 104.43 E
Area (km ²)	111.7	241.6	3892	414.4
Elevation (m a.s.l.)	0 – 2874	30 – 1778	475-2560	720-1831
Flow pattern	Parallel	Parallel (with two main river flow that meet in the downstream area)	Parallel	Radial
Land cover type	Forest (13%) Agroforest (59%) Crops (22%) Others (6%)	Forest (20%) Agroforest (32%) Crops (33%) Others (11%) Swamp(4%)	Forest (evergreen, deciduous and pine) (84%) Crops (15%) Others (1%)	Forest (18%) Coffee (monoculture and multistrata) (64%) Crop and Horticulture (12%) Others (6%)
Mean annual rainfall, mm	1695	2573	1027	2474
Wet season	April – June	January - March	July - September	January - March
Dry season	July - September	July - September	January - March	July - September
Mean annual runoff, mm	947	917	259	1673
Major soils	Inceptisols	Inceptisols	Ultisols, Entisols	Andisols

1205 Table 2. Parameters of the GenRiver model used for the four site specific simulations (van
 1206 Noordwijk et al., 2011 for definitions of terms; sequence of parameters follows the pathway of
 1207 water)

Parameter	Definition	Unit	Bialo	Cidanau	Mae Chaem	Way Besai
RainIntensMean	Average rainfall intensity	mm hr ⁻¹	30	30	3	30
RainIntensCoefVar	Coefficient of variation of rainfall intensity	mm hr ⁻¹	0.8	0.3	0.5	0.3
RainInterceptDripRt	Maximum drip rate of intercepted rain	mm hr ⁻¹	80	10	10	10
RainMaxIntDripDur	Maximum dripping duration of intercepted rain	hr	0.8	0.5	0.5	0.5
InterceptEffectontrans	Rain interception effect on transpiration	-	0.35	0.8	0.3	0.8
MaxInfRate	Maximum infiltration capacity	mm d ⁻¹	580	800	150	720
MaxInfSubsoil	Maximum infiltration capacity of the sub soil	mm d ⁻¹	80	120	150	120
PerFracMultiplier	Daily soil water drainage as fraction of groundwater release fraction	-	0.35	0.13	0.1	0.1
MaxDynGrWatStore	Dynamic groundwater storage capacity	mm	100	100	300	300
GWReleaseFracVar	Groundwater release fraction, applied to all subcatchments	-	0.15	0.03	0.05	0.1
Tortuosity	Stream shape factor	-	0.4	0.4	0.6	0.45
Dispersal Factor	Drainage density	-	0.3	0.4	0.3	0.45
River Velocity	River flow velocity	m s ⁻¹	0.4	0.7	0.35	0.5

1208

1209 Table 3. GenRiver defaults for land use specific parameter values, used for all four watersheds
1210 (BD/BDref indicates the bulk density relative to that for an agricultural soil pedotransfer
1211 function; see van Noordwijk et al., 2011)

1212

Land cover Type	Potential interception (mm/d)	Relative drought threshold	BD/BDref
Forest ¹	3.0 - 4.0	0.4 - 0.5	0.8 - 1.1
Agroforestry ²	2.0 - 3.0	0.5 - 0.6	0.95 - 1.05
Monoculture tree ³	1.0	0.55	1.08
Annual crops	1.0 - 3.0	0.6 - 0.7	1.1 - 1.5
Horticulture	1.0	0.7	1.07
Rice field ⁴	1.0 - 3.0	0.9	1.1 - 1.2
Settlement	0.05	0.01	1.3
Shrub and grass	2.0 - 3.0	0.6	1.0 - 1.07
Cleared land	1.0 - 1.5	0.3 - 0.4	1.1 - 1.2

1213 Note: 1. Forest: primary forest, secondary forest, swamp forest, evergreen forest, deciduous forest

1214 2. Agroforestry: mixed garden, coffee, cocoa, clove

1215 3. Monoculture : coffee

1216 4. Rice field: irrigation and rainfed

1217

1218 Table 4. Land use scenarios explored for four watersheds

Scenario	Description
NatFor	Full natural forest, hypothetical reference scenario
ReFor	Reforestation, replanting shrub, cleared land, grass land and some agricultural area with forest
AgFor	Agroforestry scenario, maintaining agroforestry areas and converting shrub, cleared land, grass land and some of agricultural area into agroforestry
Actual	Baseline scenario, based on the actual condition of land cover change during the modelled time period
Agric	Agriculture scenario, converting some of tree based plantations, cleared land, shrub and grass land into rice fields or dry land agriculture, while maintain existing forest
Degrading	No change in already degraded areas, while converting most of forest and agroforestry area into rice fields and dry land agriculture

1219

1220

1221 Table 5. Number of years of observations required to estimate flow persistence to reject the
 1222 null-hypothesis of ‘no land use effect’ at p-value = 0.05 using Kolmogorov-Smirnov test. The
 1223 probability of the test statistic in the first significant number is provided between brackets and
 1224 where the number of observations exceeds the time series available, results are given in *italics*

A. Natural Forest as reference

Way Besai (N=32)	ReFor	AgFor	Actual	Agric
ReFor		20 (0.035)	16 (0.037)	13 (0.046)
AgFor			n.s.	n.s.
Actual				n.s.
Agric				
Degrading				

Bialo (N=18)	ReFor	AgFor	Actual	Agric
ReFor		n.s.	n.s.	37 (0.04)
AgFor			n.s.	n.s.
Actual				n.s.
Agric				
Degrading				

Cidanau (N=20)	ReFor	AgFor	Actual	Agric
ReFor		n.s.	n.s.	32 (0.037)
AgFor			n.s.	n.s.
Actual				n.s.
Agric				
Degrading				

Mae Chaem (N=15)	ReFor	Actual	Agric	Degrad
ReFor		n.s.	23 (0.049)	18 (0.050)
Actual			45 (0.037)	33 (0.041)
Agric				33 (0.041)
Degrading				

1225

B. Degrading scenario as reference

Way Besai (N=32)	NatFor	ReFor	AgFor	Actual	Agric
NatFor		n.s.	17 (0.042)	13 (0.046)	7 (0.023)
ReFor			21 (0.037)	19 (0.026)	7 (0.023)
AgFor				n.s. 30 (0.029)	28 (0.046)
Actual					
Agric					

Bialo (N=18)	NatFor	ReFor	AgFor	Actual	Agric
NatFor		n.s.	n.s. (0.047)	41 (0.026)	19 32
ReFor			n.s.	n.s. n.s.	(0.037) n.s.
AgFor					
Actual					
Agric					

Cidanau (N=20)	NatFor	ReFor	AgFor	Actual	Agric
NatFor		n.s.	n.s. (0.041)	33 (0.034)	8 15
ReFor			n.s.	n.s. n.s.	(0.028) n.s.
AgFor					25 (0.031)
Actual					
Agric					

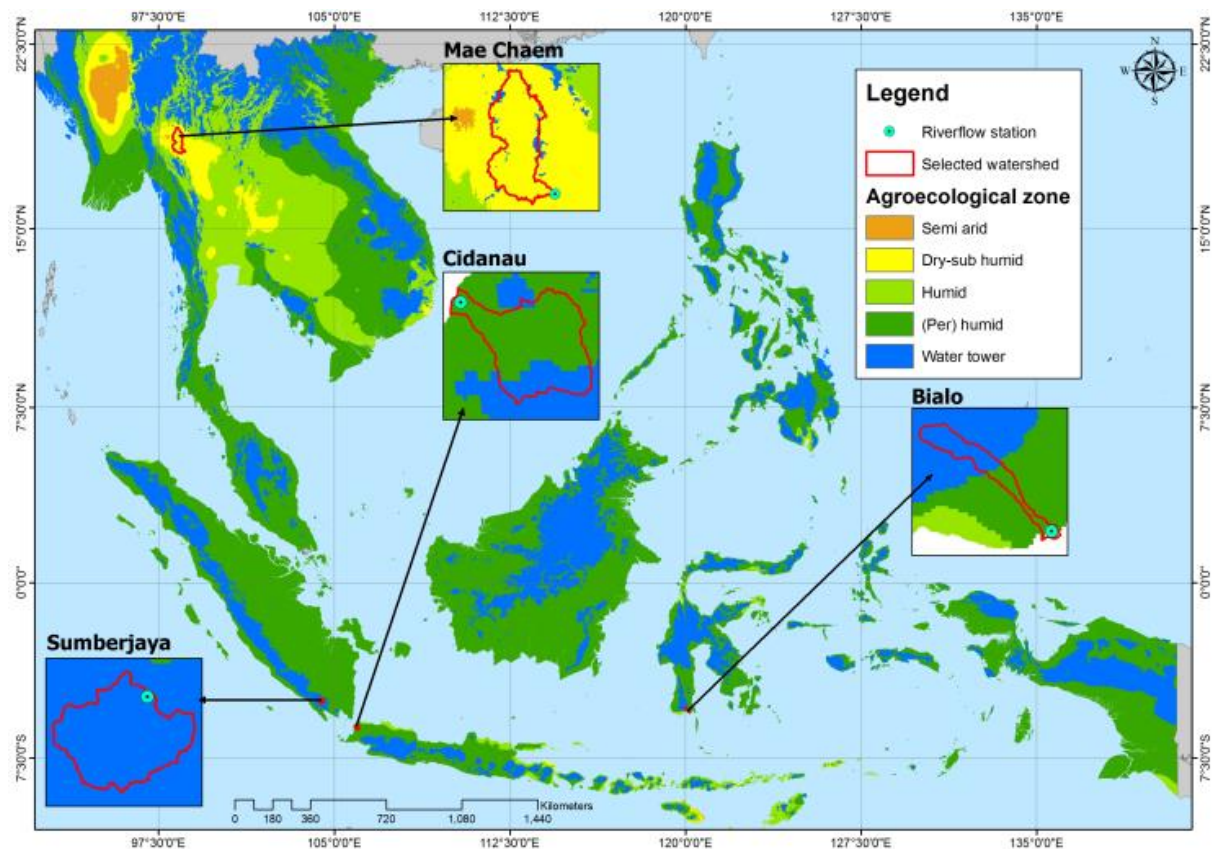
Mae Chaem (N=15)	NatFor	ReFor	Actual	Agric
NatFor		n.s.	25 (0.031)	12 (0.037)
ReFor			n.s. n.s.	18 (0.050)
Actual				18 (0.050)
Agric				

1227 Table 6. Data availability

	Bialo	Cidanau	Mae Chaem	Way Besai
Rainfall data	1989-2009, Source: BWS Sulawesi ^a and PUSAIR ^b ; Average rainfall data from the stations Moti, Bulo-bulo, Seka and Onto	1998-2008, source: BMKG ^c	1998-2002, source: WRD55, MTD22, RYP48, GMT13, WRD 52	1976-2007, Source: BMKG, PU ^d and PLN ^e (interpolation of 8 rainfall stations using Thiessen polygon)
River flow data	1993-2010, source: BWS Sulawesi and PUSAIR	2000-2009, source: KTI ^f	1954-2003, source: ICHARM ^g	1976-1998, source: PU and PUSAIR
Reference of detailed report	http://old.icraf.org/regions/southeast_asia/publications?do=view_pub_detail&pub_no=PP0343-14	http://worldagroforestry.org/regions/southeast_asia/publications?do=view_pub_detail&pub_no=PO0292-13	http://worldagroforestry.org/regions/south_east_asia/publications?do=view_pub_detail&pub_no=MN0048-11	http://worldagroforestry.org/regions/southeast_asia/publications?do=view_pub_detail&pub_no=MN0048-11

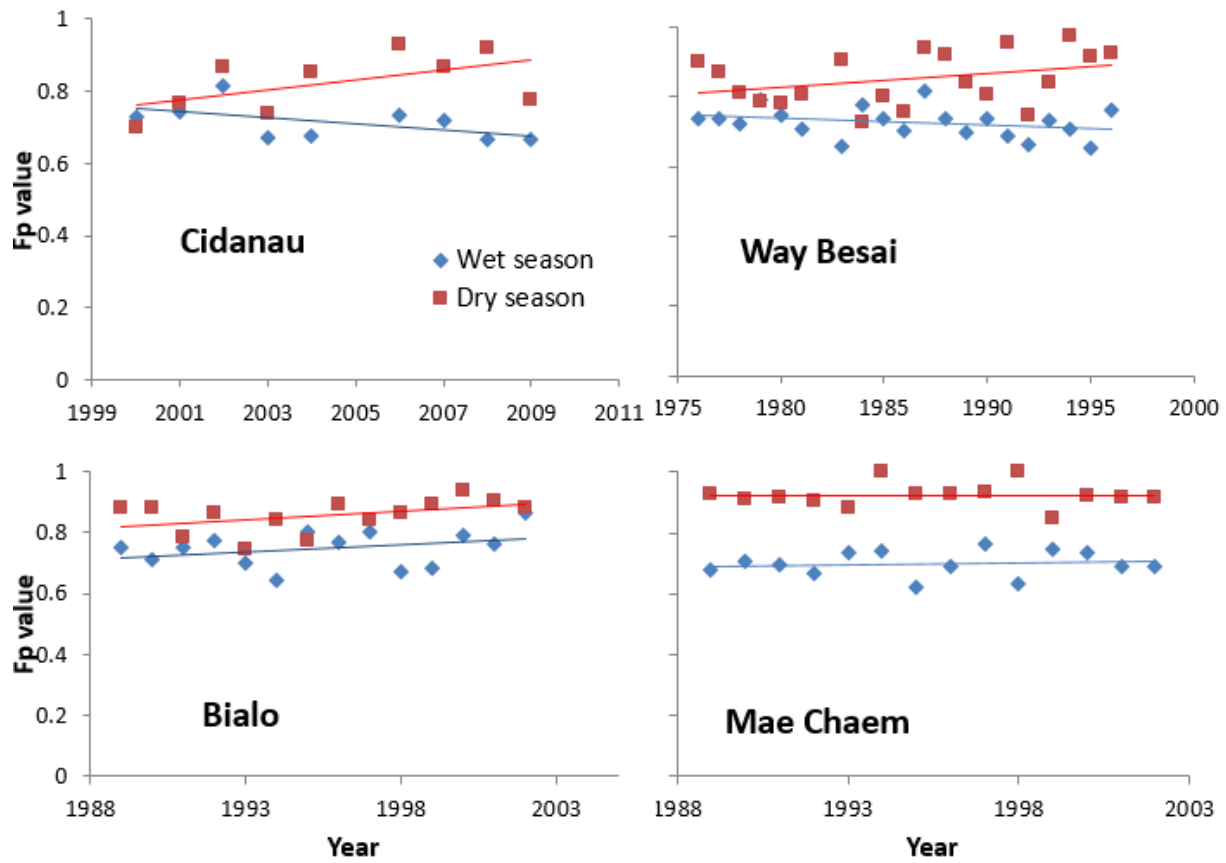
1228 Note:

1229 ^aBWS: Balai Wilayah Sungai (*Regional River Agency*)1230 ^bPUSAIR: Pusat Litbang Sumber Daya Air (*Centre for Research and Development on Water Resources*)1232 ^cBMKG: Badan Meteorologi Klimatologi dan Geofisika (*Agency on Meterology, Climatology and Geophysics*)1234 ^dPU: Dinas Pekerjaan Umum (*Public Work Agency*)1235 ^ePLN: Perusahaan Listrik Negara (*National Electric Company*)1236 ^fKTI: Krakatau Tirta Industri, a private steel company1237 ^gICHARM: The International Centre for Water Hazard and Risk Management



1240 Figure 1. Location of the four watersheds in the agroecological zones of Southeast Asia (water
 1241 towers are defined on the basis of ability to generate river flow and being in the upper part
 1242 of a watershed)

1244



1245

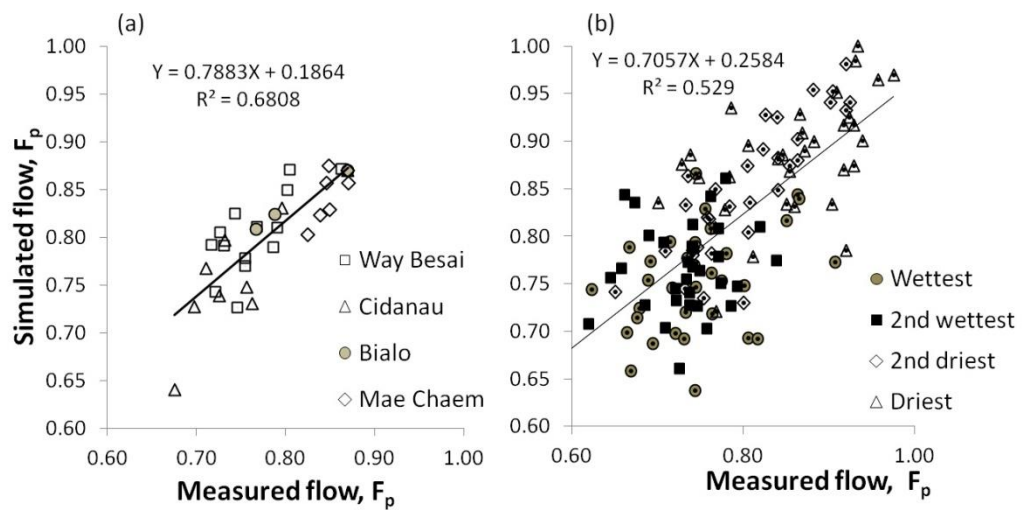
Figure 2. Flow persistence (F_p) estimates derived from measurements in four watersheds, separately for the wettest and driest 3-month periods of the year

1246

1247

1248

1249

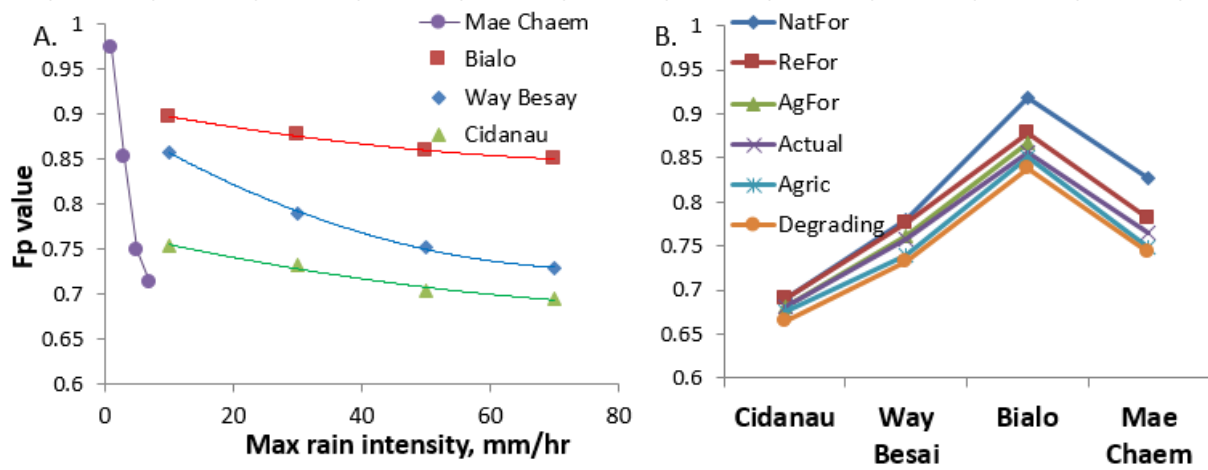


1250

1251 Figure 3. Inter- (A) and intra- (B) annual variation in the F_p parameter derived from empirical
1252 versus modeled flow: for the four test sites on annual basis (A) or three-monthly basis (B)

1253

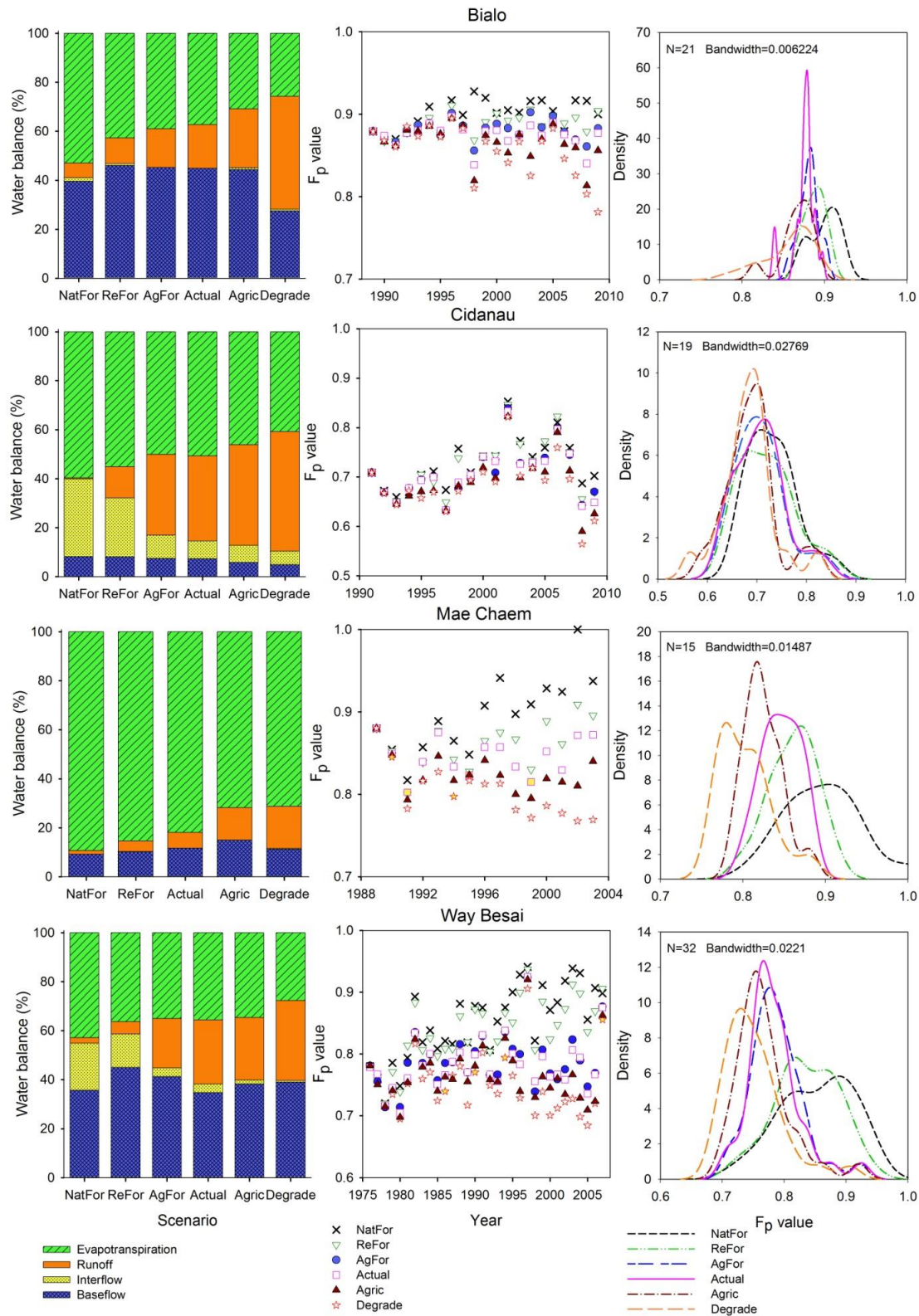
1254



1255

1256 Figure 4 Effects on flow persistence of changes in A) the mean rainfall intensity and B) the land
1257 use change scenarios of Table 4 across the four watersheds

1258

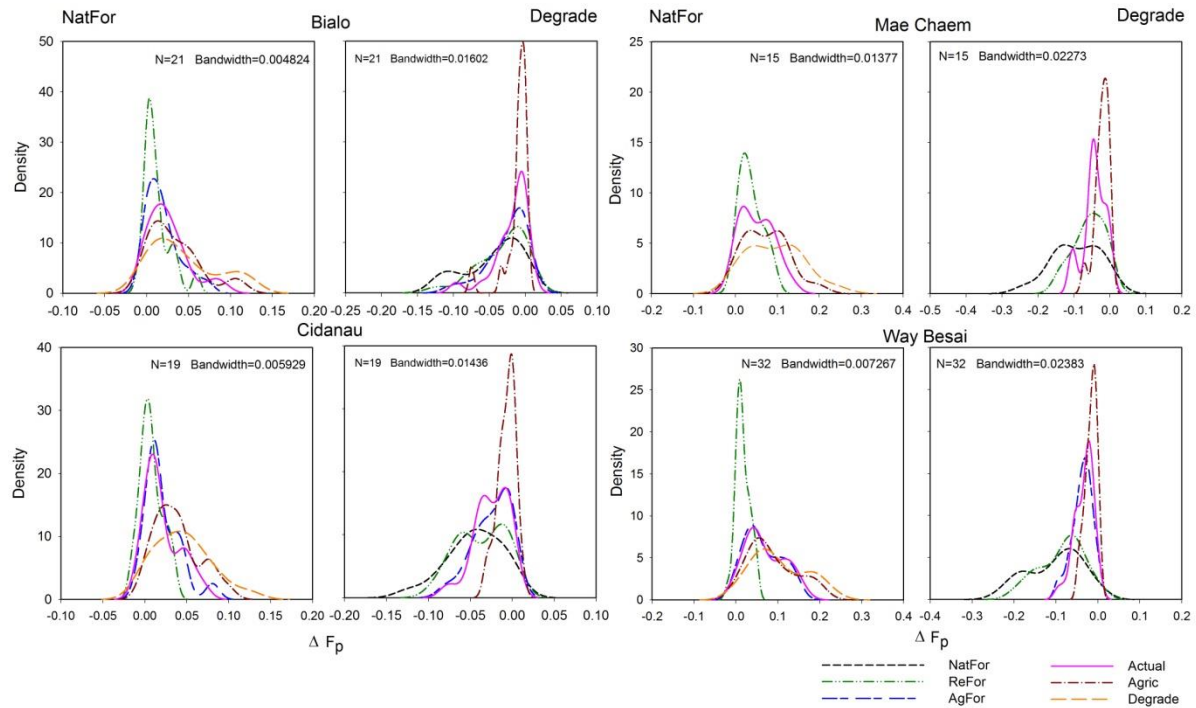


1259

1260 Figure 5. Effects of land cover change scenarios (Table 4) on the flow persistence value in four
 1261 watersheds, modelled in GenRiver over a 20-year time-period, based on actual rainfall
 1262 records; the left side panels show average water balance for each land cover scenario, the

1263 middle panels the F_p values per year and land use, the right-side panels the derived frequency
1264 distributions (best fitting Weibull distribution)

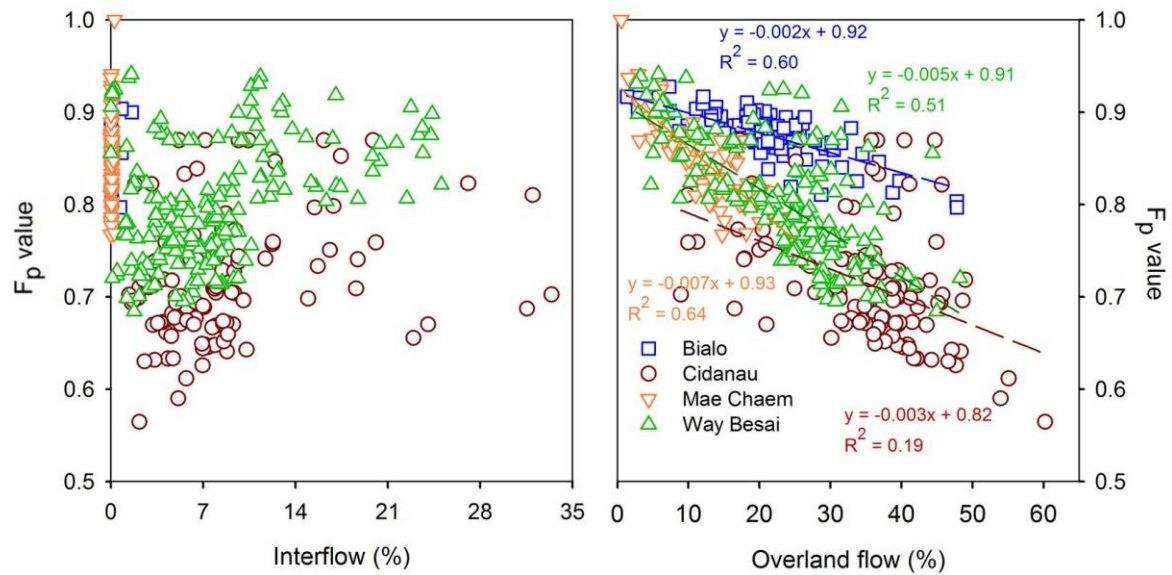
1265



1266

1267 Figure 6. Frequency distribution of expected difference in F_p in 'paired plot' comparisons where
1268 land cover is the only variable; left panels: all scenarios compared to 'reforestation', right
1269 panel: all scenarios compared to degradation; graphs are based on a kernel density estimation
1270 (smoothing) approach

1271



1272

1273 Figure 7. Correlations of F_p with fractions of rainfall that take overland flow and interflow
1274 pathways through the watershed, across all years and land use scenarios of Figure App2
1275
1276

1277 Appendix 1. GenRiver model for effects of land cover on river flow

1278 The Generic River flow (GenRiver) model (van Noordwijk et al., 2011) is a simple hydrological
 1279 model that simulates river flow based on water balance concept with a daily time step and a
 1280 flexible spatial subdivision of a watershed that influences the routing of water. The core of the
 1281 GenRiver model is a “patch” level representation of a daily water balance, driven by local
 1282 rainfall and modified by the land cover and land cover change and soil properties. The model
 1283 starts accounting of rainfall or precipitation (P) and traces the subsequent flows and storage in
 1284 the landscape that can lead to either evapotranspiration (E), river flow (Q) or change in storage
 1285 (ΔS) (Figure App1):

1286 $P = Q + E + \Delta S$ [1]

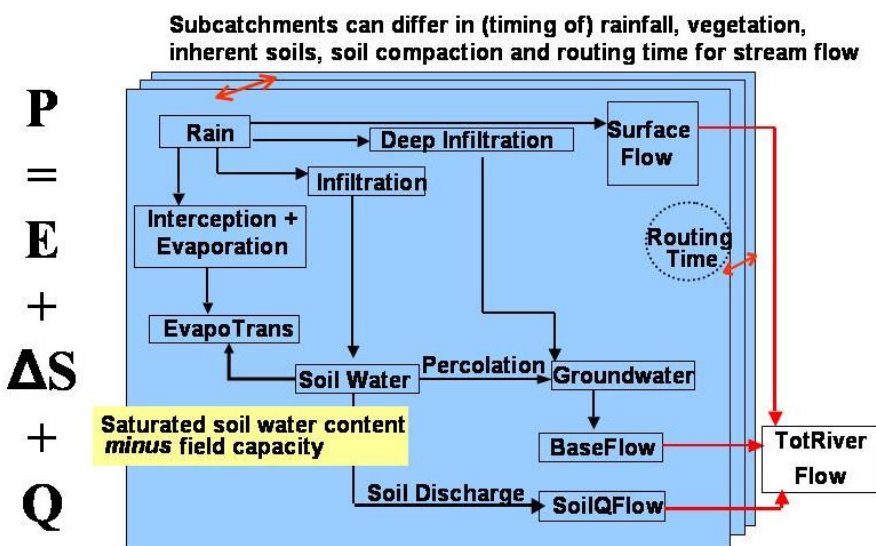


Figure App1.Overview of the GenRiver model

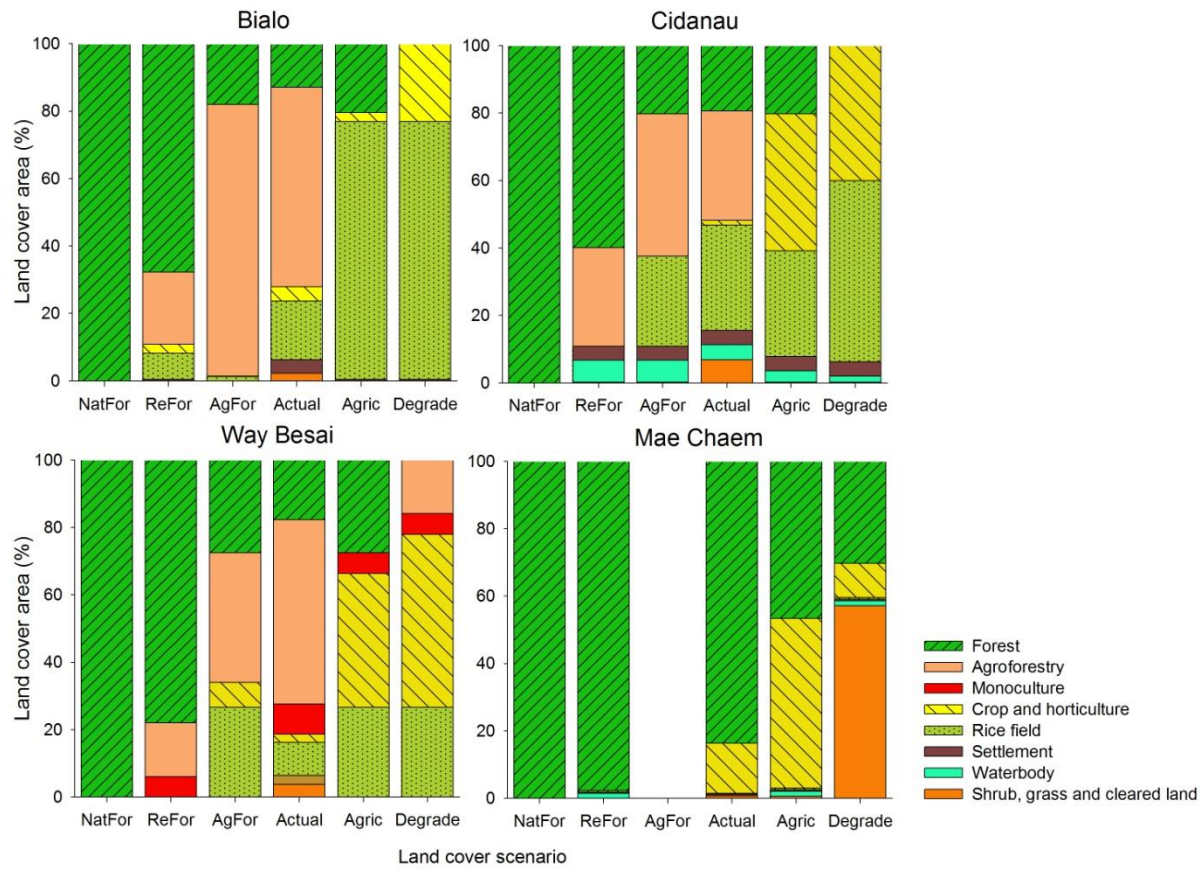
1287

1288 The model may use measured rainfall data, or use a rainfall generator that involves Markov
 1289 chain temporal autocorrelation (rain persistence). The model can represent spatially explicit
 1290 rainfall, with stochastic rainfall intensity (parameters RainIntensMean, RainIntensCoefVar in Table
 1291 2) and partial spatial correlation of daily rainfall between subcatchments. Canopy interception
 1292 leads to direct evaporation of an amount of water controlled by the thickness of waterfilm on
 1293 the leaf area that depends on the land cover, and a delay of water reaching the soil surface
 1294 (parameter RainMaxIntDripDur in Table 2). The effect of evaporation of intercepted water on other
 1295 components of evapotranspiration is controlled by the InterceptEffectontrans parameter, that in practice
 1296 may depend on the time of day rainfall occurs and local climatic conditions such as windspeed)

1297 At patch level, vegetation influences interception, retention for subsequent evaporation and
1298 delayed transfer to the soil surface, as well as the seasonal demand for water. Vegetation (land
1299 cover) also influences soil porosity and infiltration, modifying the inherent soil properties.
1300 Groundwater pool dynamics are represented at subcatchment rather than patch level, integrating
1301 over the landcover fractions within a subcatchment. The output of the model is river flow which
1302 is contribution from three types of stream flow: surface flow on the day of the rainfall event;
1303 interflow on the next day; and base flow as the slow flow. the multiple subcatchments that make
1304 up the catchment as a whole can differ in basic soil properties, land cover fractions that affect
1305 interception, soil structure (infiltration rate) and seasonal pattern of water use by the vegetation.
1306 The subcatchment will also typically differ in “routing time” or in the time it takes the streams
1307 and river to reach any specified observation point (with default focus on the outflow from the
1308 catchment). The model itself (currently implemented in Stella plus Excel), a manual and
1309 application case studies are freely available
1310 (<http://www.worldagroforestry.org/output/genriver-genetic-river-model-river-flow> ;van
1311 Noordwijk et al., 2011).
1312

1313 Appendix 2. Watershed-specific consequences of the land use change scenarios

1314 The generically defined land use change scenarios (Table 4) led to different land cover
1315 proportions, depending on the default land cover data for each watershed, as shown in Figure
1316 App2.



1317
1318 Figure App2. Land use distribution of the various land use scenarios explored for the four
1319 watersheds (see Table 4)

1320

1321 Appendix 3. Example of a macro in R to estimate number of observation required using
1322 bootstrap approach.

1323

```
1324 #The bootstrap procedure is to calculate the minimum sample size (number of observation) required
1325 #for a significant land use effect on Fp
1326 #bialo1 is a dataset contains delta Fp values for two different from Bialo watershed
1327
1328 #read data
1329 bialo1 <- read.table("bialo1.csv", header=TRUE, sep=",")
1330
1331 #name each parameter
1332 BL1 <- bialo1$ReFor
1333 BL5 <- bialo1$Degrade
1334
1335 N = 1000 #number replication
1336
1337 n <- c(5:50) #the various sample size
1338
1339 J <- 46 #the number of sample size being tested (~ number of actual year observed in the dataset)
1340
1341 P15= matrix(ncol=J, nrow=R) #variable for storing p-value
1342 P15Q3 <- numeric(J) #for storing p-Value at 97.5 quantile
1343
1344 for (j in 1:J) #estimating for different n
1345
1346 #bootstrap sampling
1347 {
1348 for (i in 1:N)
1349 {
1350 #sampling data
1351 S1=sample(BL1, n[j], replace = T)
1352 S5=sample(BL5, n[j], replace = T)
1353
1354 #Kolmogorov-Smirnov test for equal distribution and get the p-Value
1355 KS15 <- ks.test(S1, S5, alt = c("two.sided"), exact = F) P15[i,j] <- KS15$p.value
1356 }
1357
1358 #Confidence interval of CI
1359 P15Q3[j] <- quantile(P15[,j], 0.975)
1360
1361 }
1362
1363 #saving P value data and CI
1364
1365 write.table(P15, file = "pValue15.txt") write.table(P15Q3, file = "P15Q3.txt")v
```